

Fitting the seven-parameter Generalized Tempered Stable distribution to the financial data

Aubain Nzokem and Daniel Maposa

*Corresponding author(s). E-mail(s): hilaire77@gmail.com;

Abstract

The paper proposes and implements a methodology to fit a seven-parameter Generalized Tempered Stable (GTS) distribution to financial data. The nonexistence of the mathematical expression of the GTS probability density function makes the maximum likelihood estimation (MLE) inadequate for providing parameter estimations. Based on the function characteristic and the fractional Fourier transform (FRFT), we provide a comprehensive approach to circumvent the problem and yield a good parameter estimation of the GTS probability. The methodology was applied to fit two heavily tailed data (Bitcoin and Ethereum returns) and two peaked data (S&P 500 and SPY ETF returns). For each index, the estimation results show that the six-parameter estimations are statistically significant except for the local parameter, μ . The goodness-of-fit was assessed through Kolmogorov-Smirnov, Anderson-Darling, and Pearson's chi-squared statistics. While the two-parameter geometric Brownian motion (GBM) hypothesis is always rejected, the GTS distribution fits significantly with a very high p-value; and outperforms the Kobol, Carr-Geman-Madan-Yor, and Bilateral Gamma distributions.

Keywords: Generalized Tempered Stable (GTS), Fractional Fourier Transform (FRFT), Function Characteristic, Kolmogorov-Smirnov (K-S), Maximum Likelihood Estimation (MLE)

1 Introduction

Modeling the high-frequency asset return with the normal distribution is the underlying assumption in many financial tools, such as the Black-Scholes-Merton option pricing model and the risk metric variance-covariance technique to Value-at-Risk (VAR). However, substantial empirical evidence rejects the normal distribution for various asset classes and financial markets. The symmetric and rapidly decreasing

tail properties of the normal distribution cannot describe the skewed and fat-tailed properties of the asset return distribution.

The α -stable distribution has been proposed [1, 2] as an alternative to the normal distribution for modeling asset return and many types of physical and economic systems. The theoretical and empirical argument is that the stable distribution generalizes the Central Limit Theorem regardless of the variance nature (finite or infinite)[3, 4]. There are two major drawbacks [2, 5]: firstly, the lack of closed formulas for densities and distribution functions, except for the normal distribution ($\alpha = 2$), Cauchy distribution ($\alpha = 1$) and Lévy distribution ($\alpha = \frac{1}{2}$)[6]; secondly, most of the moments of the stable distribution are infinite. An infinite variance of the asset return leads to an infinite price for derivative instruments such as options.

The Generalized Tempered Stable (GTS) distribution was developed to overcome the shortcomings of the two distributions, and the tails of the GTS distribution are heavier than the normal distribution but thinner than the stable distribution[7, 8]. The general form of the GTS distribution can be defined by the following Lévy measure ($V(dx)$) (1):

$$V(dx) = \left(\frac{\alpha_+ e^{-\lambda_+ x}}{x^{1+\beta_+}} \mathbf{1}_{x>0} + \frac{\alpha_- e^{-\lambda_- |x|}}{|x|^{1+\beta_-}} \mathbf{1}_{x<0} \right) dx \quad (1)$$

where $0 \leq \beta_+ \leq 1$, $0 \leq \beta_- \leq 1$, $\alpha_+ \geq 0$, $\alpha_- \geq 0$, $\lambda_+ \geq 0$ and $\lambda_- \geq 0$. More details on Tempered Stable distribution are provided [3, 9].

The rich class of GTS distribution (1) has a myriad of applications ranging from financial to mathematical physics and economic systems. However, few studies [10–12] have covered the methods and techniques to estimate the parameters of the GTS distribution. This study aims to contribute to the literature by providing a methodology for fitting seven-parameter GTS distribution. As illustrations, the study used four historical prices: two heavily tailed data (Bitcoin and Ethereum returns) and two peaked data (S&P 500 and SPY ETF returns). The GTS distribution is fitted to the underlying distribution of each data index and the goodness-of-fit analysis is carried out. The main disadvantage of the GTS distribution is the lack of the closed form of the density, cumulative, and derivative functions. We use a computational algorithm, called the enhanced fast FRFT scheme [13], to circumvent the problem.

The rest of the paper is organized as follows: Section 2 provides some theoretical framework of the GTS distribution. Section 3 presents the multivariate maximum likelihood (ML) method and the analytic version of the two-parameter normal distribution. Section 4 presents the results of the GTS parameter estimations along with the associated statistical tests for the heavily-tailed Bitcoin and Ethereum returns. Section 5 fits the GTS distribution to the traditional indices S&P 500 and SPY ETF returns, while Section 6 presents the results of the goodness-of-fit test. Section 7 provides the concluding remarks.

2 Generalized Tempered Stable (GTS) Distribution

The Lévy measure of the GTS distribution ($V(dx)$) is defined in (2) as a product of a tempering function $q(x)$ and a Lévy measure of the α -stable distribution $V_{stable}(dx)$:

$$\begin{aligned} q(x) &= e^{-\lambda_+ x} \mathbf{1}_{x>0} + e^{-\lambda_- |x|} \mathbf{1}_{x<0} \\ V_{stable}(dx) &= \left(\alpha_+ \frac{1}{x^{1+\beta_+}} \mathbf{1}_{x>0} + \alpha_- \frac{1}{|x|^{1+\beta_-}} \mathbf{1}_{x<0} \right) dx \\ V(dx) &= q(x) V_{stable}(dx) = \left(\alpha_+ \frac{e^{-\lambda_+ x}}{x^{1+\beta_+}} \mathbf{1}_{x>0} + \alpha_- \frac{e^{-\lambda_- |x|}}{|x|^{1+\beta_-}} \mathbf{1}_{x<0} \right) dx \end{aligned} \quad (2)$$

where $0 \leq \beta_+ \leq 1$, $0 \leq \beta_- \leq 1$, $\alpha_+ \geq 0$, $\alpha_- \geq 0$, $\lambda_+ \geq 0$ and $\lambda_- \geq 0$.

The six parameters that appear have important interpretations. β_+ and β_- are the indexes of stability bounded below by 0 and above by 2 [5]. They capture the peakedness of the distribution similarly to the β -stable distribution, but the distribution tails are tempered. If β increases (decreases), then the peakedness decreases (increases). α_+ and α_- are the scale parameters, also called the process intensity [14]; they determine the arrival rate of jumps for a given size. λ_+ and λ_- control the decay rate on the positive and negative tails. Additionally, λ_+ and λ_- are also skewness parameters. If $\lambda_+ > \lambda_-$ ($\lambda_+ < \lambda_-$), then the distribution is skewed to the left (right), and if $\lambda_+ = \lambda_-$, then it is symmetric [3, 15]. α and λ are related to the degree of peakedness and thickness of the distribution. If α increases (decreases), the peakedness and the thickness decrease (increase). Similarly, if λ increases (decreases), then the peakedness increases (decreases) and the thickness decreases (increases) [16]. For more details on tempering function and Lévy measure of tempered stable distribution, refer to [3, 9].

The activity process of the GTS distribution can be studied from the integral (3) of the Lévy measure (2):

$$\int_{-\infty}^{+\infty} V(dx) = \begin{cases} +\infty & \text{if } 0 \leq \beta_+ < 1 \wedge 0 \leq \beta_- < 1 \\ \alpha_+ \lambda_+^{\beta_+} \Gamma(-\beta_+) + \alpha_- \lambda_-^{\beta_-} \Gamma(-\beta_-) & \text{if } \beta_+ < 0 \wedge \beta_- < 0. \end{cases} \quad (3)$$

As shown in (3), if $\beta_+ < 0$ and $\beta_- < 0$, $GTS(\beta_+, \beta_-, \alpha_+, \alpha_-, \lambda_+, \lambda_-)$ is of finite activity process and can be written as a compound Poisson [17]. When $0 \leq \beta_+ < 1$ and $0 \leq \beta_- < 1$, this Lévy density ($V(dx)$) is not integrable as it goes off to infinity too rapidly as x goes to zero [17], which means in practice that there will be a large number of very small jumps. As shown in (3), $GTS(\beta_+, \beta_-, \alpha_+, \alpha_-, \lambda_+, \lambda_-)$ is an infinite activity process with infinite jumps in any given time interval.

In addition to the infinite activities process, the variation of the process can be studied through the following integral:

$$\begin{aligned} \int_{-1}^1 |x| V(dx) &= \int_{-1}^0 |x| V(dx) + \int_0^1 |x| V(dx) \\ &= \alpha_- \lambda_-^{\beta_- - 1} \gamma(1 - \beta_-, \lambda_-) + \alpha_+ \lambda_+^{\beta_+ - 1} \gamma(1 - \beta_+, \lambda_+) \end{aligned}$$

where $\gamma(s, x) = \int_0^x y^{s-1} e^{-y} dy$ is the lower incomplete gamma function.

And we have:

$$\int_{-1}^1 |x|V(dx) < +\infty \quad \text{if } 0 < \beta_- \leq 1 \text{ \& } 0 < \beta_+ \leq 1. \quad (4)$$

As shown in (4), $GTS(\beta_+, \beta_-, \alpha_+, \alpha_-, \lambda_+, \lambda_-)$ generates a finite variance process, which is contrary to the Brownian motion process. $GTS(\beta_+, \beta_-, \alpha_+, \alpha_-, \lambda_+, \lambda_-)$ generates a type B Lévy process [18], which is a purely non-Gaussian infinite activity Lévy process of finite variation whose sample paths have an infinite number of small jumps and a finite number of large jumps in any finite time interval.

The GTS distribution can be denoted by $X \sim GTS(\beta_+, \beta_-, \alpha_+, \alpha_-, \lambda_+, \lambda_-)$ and $X = X_+ - X_-$ with $X_+ \geq 0$, $X_- \geq 0$. $X_+ \sim TS(\beta_+, \alpha_+, \lambda_+)$ and $X_- \sim TS(\beta_-, \alpha_-, \lambda_-)$. By adding the location parameter, the GTS distribution becomes $GTS(\mu, \beta_+, \beta_-, \alpha_+, \alpha_-, \lambda_+, \lambda_-)$, and we have (5):

$$Y = \mu + X = \mu + X_+ - X_-, \quad Y \sim GTS(\mu, \beta_+, \beta_-, \alpha_+, \alpha_-, \lambda_+, \lambda_-). \quad (5)$$

2.1 GTS Distribution and Characteristic Exponent

Theorem 1.

Consider a variable $Y \sim GTS(\mu, \beta_+, \beta_-, \alpha_+, \alpha_-, \lambda_+, \lambda_-)$. The characteristic exponent can be written as:

$$\Psi(\xi) = \mu\xi + \alpha_+ \Gamma(-\beta_+) \left((\lambda_+ - i\xi)^{\beta_+} - \lambda_+^{\beta_+} \right) + \alpha_- \Gamma(-\beta_-) \left((\lambda_- + i\xi)^{\beta_-} - \lambda_-^{\beta_-} \right). \quad (6)$$

Proof.

$V(dx)$ in (2) is a Lévy measure. The following relation is satisfied from (4):

$$\int_{-\infty}^{+\infty} \text{Min}(1, |x|)V(dx) < +\infty.$$

More details on the proof are provided in [19].

The Lévy-Khintchine representation [17] for non-negative Lévy process is applied on Y . $Y = \mu + X = \mu + X_+ - X_-$ and we have:

$$\begin{aligned} \Psi(\xi) &= \text{Log} (Ee^{iY\xi}) = i\mu\xi + \text{Log} (Ee^{iX_+\xi}) + \text{Log} (Ee^{-iX_-\xi}) \\ &= i\mu\xi + \int_0^{+\infty} (e^{iy\xi} - 1) \frac{\alpha_+ e^{-\lambda_+ y}}{y^{1+\beta_+}} dy + \int_0^{+\infty} (e^{-iy\xi} - 1) \frac{\alpha_- e^{-\lambda_- y}}{y^{1+\beta_-}} dy, \end{aligned} \quad (7)$$

$$\begin{aligned}
\int_0^{+\infty} (e^{iy\xi} - 1) \frac{\alpha_+ e^{-\lambda_+ y}}{y^{1+\beta_+}} dy &= \alpha_+ \lambda_+^{\beta_+} \Gamma(-\beta_+) \sum_{k=1}^{+\infty} \frac{\Gamma(k - \beta_+)}{\Gamma(-\beta_+) k!} \left(\frac{i\xi}{\lambda_+}\right)^k \\
&= \alpha_+ \lambda_+^{\beta_+} \Gamma(-\beta_+) \sum_{k=1}^{+\infty} \binom{\beta_+}{k} \left(-\frac{i\xi}{\lambda_+}\right)^k \\
&= \alpha_+ \Gamma(-\beta_+) \left((\lambda_+ - i\xi)^{\beta_+} - \lambda_+^{\beta_+}\right).
\end{aligned} \tag{8}$$

Similarly, we have :

$$\int_0^{+\infty} (e^{-iy\xi} - 1) \frac{\alpha_- e^{-\lambda_- y}}{y^{1+\beta_-}} dy = \alpha_- \Gamma(-\beta_-) \left((\lambda_- + i\xi)^{\beta_-} - \lambda_-^{\beta_-}\right). \tag{9}$$

The expression in (7) becomes:

$$\Psi(\xi) = i\mu\xi + \alpha_+ \Gamma(-\beta_+) \left((\lambda_+ - i\xi)^{\beta_+} - \lambda_+^{\beta_+}\right) + \alpha_- \Gamma(-\beta_-) \left((\lambda_- + i\xi)^{\beta_-} - \lambda_-^{\beta_-}\right).$$

□

Theorem 2.

Consider a variable $Y \sim GTS(\mu, \beta_+, \beta_-, \alpha_+, \alpha_-, \lambda_+, \lambda_-)$.

If $(\beta_-, \beta_+) \rightarrow (0, 0)$, GTS becomes a *Bilateral Gamma distribution* with the following characteristic exponent:

$$\Psi(\xi) = \mu\xi i - \alpha_+ \log\left(1 - \frac{1}{\lambda_+} i\xi\right) - \alpha_- \log\left(1 + \frac{1}{\lambda_-} i\xi\right). \tag{10}$$

In addition to $(\beta_-, \beta_+) \rightarrow (0, 0)$, if $\alpha_- = \alpha_+ = \alpha$, GTS becomes *Variance-Gamma (VG) distribution* with parameter $(\mu, \delta, \sigma, \alpha, \theta)$

$$\delta = \lambda_- - \lambda_+ \quad \sigma = 1 \quad \alpha = \alpha_- = \alpha_+ \quad \theta = \frac{1}{\lambda_- \lambda_+}$$

and the following characteristic exponent:

$$\Psi(\xi) = \mu\xi i - \alpha \log\left(1 - \frac{\lambda_- - \lambda_+}{\lambda_+ \lambda_-} i\xi + \frac{1}{\lambda_+ \lambda_-} \xi^2\right). \tag{11}$$

Proof.

$$\Gamma(-\beta_+) = -\frac{\Gamma(1 - \beta_+)}{\beta_+} \tag{12}$$

$$\lim_{\beta_+ \rightarrow 0} \Gamma(-\beta_+) \left((\lambda_+ - i\xi)^{\beta_+} - \lambda_+^{\beta_+}\right) = -\log\left(1 - \frac{1}{\lambda_+} i\xi\right).$$

Similarly, (12) works for $\beta_- \rightarrow 0$, and we have the characteristic exponent (10).

In addition, if $\alpha_- = \alpha_+ = \alpha$, from (10), the characteristic exponent becomes:

$$\Psi(\xi) = \mu\xi i - \alpha \log \left(1 - \frac{\lambda_- - \lambda_+}{\lambda_+ \lambda_-} i\xi + \frac{1}{\lambda_+ \lambda_-} \xi^2 \right),$$

which is a Variance-Gamma (VG) distribution with parameter $(\mu, \lambda_- - \lambda_+, 1, \alpha, \frac{1}{\lambda_- \lambda_+})$. For more details on the VG model, refer to [20, 21]. \square

Theorem 3. (Cumulants κ_k)

Consider a variable $Y \sim GTS(\mu, \beta_+, \beta_-, \alpha_+, \alpha_-, \lambda_+, \lambda_-)$. The cumulants κ_k of the GTS distribution are defined as follows:

$$\begin{aligned} \kappa_0 &= 0 \\ \kappa_1 &= \mu + \alpha_+ \frac{\Gamma(1 - \beta_+)}{\lambda_+^{1 - \beta_+}} - \alpha_- \frac{\Gamma(1 - \beta_-)}{\lambda_-^{1 - \beta_-}} \\ \kappa_k &= \alpha_+ \frac{\Gamma(k - \beta_+)}{\lambda_+^{k - \beta_+}} + (-1)^k \alpha_- \frac{\Gamma(k - \beta_-)}{\lambda_-^{k - \beta_-}} \quad \forall k \in \mathbb{N} \setminus \{0, 1\}. \end{aligned} \quad (13)$$

Proof.

We reconsider the characteristic exponent $\Psi(\xi)$ in (7):

$$\begin{aligned} \Psi(\xi) &= i\mu\xi + \int_0^{+\infty} (e^{iy\xi} - 1) \frac{\alpha_+ e^{-\lambda_+ y}}{y^{1 + \beta_+}} dy + \int_0^{+\infty} (e^{-iy\xi} - 1) \frac{\alpha_- e^{-\lambda_- y}}{y^{1 + \beta_-}} dy \\ &= i\mu\xi + \alpha_+ \sum_{k=1}^{+\infty} \frac{\Gamma(k - \beta_+)}{\lambda_+^{k - \beta_+}} \frac{(i\xi)^k}{k!} + \alpha_- \sum_{k=1}^{+\infty} \frac{\Gamma(k - \beta_-)}{\lambda_-^{k - \beta_-}} \frac{(-i\xi)^k}{k!} \\ &= i\mu\xi + \sum_{k=1}^{+\infty} \frac{1}{k!} \left(\alpha_+ \frac{\Gamma(k - \beta_+)}{\lambda_+^{k - \beta_+}} + \alpha_- \frac{\Gamma(k - \beta_-)}{\lambda_-^{k - \beta_-}} (-1)^k \right) (i\xi)^k \\ &= \sum_{k=0}^{+\infty} \frac{\kappa_k}{k!} (i\xi)^k. \end{aligned} \quad (14)$$

Hence, the k -th order cumulant κ_k is given by comparing the coefficients of both polynomial functions in $i\xi$. For more details on the relationship between the characteristic exponent and cumulant functions, refer to [22, 23]. \square

2.2 GTS Distribution and Lévy Process

Corollary 4.

Let $Y = (Y_t)$ be a Lévy process on \mathbb{R}^+ generated by $GTS(\mu, \beta_+, \beta_-, \alpha_+, \alpha_-, \lambda_+, \lambda_-)$, then

$$Y_t \sim GTS(t\mu, \beta_+, \beta_-, t\alpha_+, t\alpha_-, \lambda_+, \lambda_-) \quad \forall t \in \mathbb{R}^+. \quad (15)$$

Proof.

Let $\Psi(\xi, t)$ be the characteristic exponent of the Lévy process $Y = (Y_t)$. By applying

the infinitely divisible property, we have:

$$\begin{aligned}\Psi(\xi, t) &= \text{Log} (Ee^{iY_t\xi}) = t\text{Log} (Ee^{iX\xi}) \\ &= t\mu\xi i + t\alpha_+\Gamma(-\beta_+) \left((\lambda_+ - i\xi)^{\beta_+} - \lambda_+^{\beta_+} \right) + t\alpha_-\Gamma(-\beta_-) \left((\lambda_- + i\xi)^{\beta_-} - \lambda_-^{\beta_-} \right)\end{aligned}$$

and we deduce that $Y_t \sim GTS(t\mu, \beta_+, \beta_-, t\alpha_+, t\alpha_-, \lambda_+, \lambda_-)$. \square

Theorem 5. (*Asymptotic distribution of Generalized Tempered Stable distribution process*)

Let $Y = Y_t$ be a Lévy process on \mathbb{R} generated by $GTS(\mu, \beta_+, \beta_-, \alpha_+, \alpha_-, \lambda_+, \lambda_-)$. Then Y_t converges in distribution to a Lévy process driving by a normal distribution with mean κ_1 and variance κ_2

$$Y_t \xrightarrow{d} N(t\kappa_1, t\kappa_2) \quad \text{as } t \rightarrow +\infty \quad (16)$$

where

$$\begin{aligned}\kappa_1 &= \mu + \alpha_+ \frac{\Gamma(1 - \beta_+)}{\lambda_+^{1 - \beta_+}} - \alpha_- \frac{\Gamma(1 - \beta_-)}{\lambda_-^{1 - \beta_-}} \\ \kappa_2 &= \alpha_+ \frac{\Gamma(2 - \beta_+)}{\lambda_+^{2 - \beta_+}} + \alpha_- \frac{\Gamma(2 - \beta_-)}{\lambda_-^{2 - \beta_-}}.\end{aligned}$$

Proof.

The proof relies on the cumulant-generating function. As in (14), the characteristic exponent ($\Psi(\xi)$) can be written as follows:

$$\Psi(\xi) = \text{Log} (Ee^{iY\xi}) = \sum_{j=0}^{+\infty} \kappa_j \frac{(i\xi)^j}{j!}. \quad (17)$$

Let $\phi(\xi, t)$ be the characteristic function of the stochastic process $\frac{Y_t - t\kappa_1}{\sqrt{t\kappa_2}}$ and we have:

$$\begin{aligned}\phi(\xi, t) &= E \left(e^{i \frac{Y_t - t\kappa_1}{\sqrt{t\kappa_2}} \xi} \right) = e^{-i \frac{t\kappa_1}{\sqrt{t\kappa_2}} \xi} E \left(e^{i \frac{\xi}{\sqrt{t\kappa_2}} Y_t} \right) \\ &= e^{-i \frac{t\kappa_1}{\sqrt{t\kappa_2}} \xi} e^{t\Psi\left(\frac{\xi}{\sqrt{t\kappa_2}}\right)} = e^{-i \frac{t\kappa_1}{\sqrt{t\kappa_2}} \xi} e^{\sum_{j=0}^{+\infty} \frac{t\kappa_j}{j!} \left(i \frac{\xi}{\sqrt{t\kappa_2}}\right)^j} \\ &= e^{-\frac{\xi^2}{2} + \sum_{j=3}^{+\infty} \frac{t\kappa_j}{j!} \left(i \frac{\xi}{\sqrt{t\kappa_2}}\right)^j},\end{aligned} \quad (18)$$

$$\begin{aligned}\lim_{t \rightarrow +\infty} \sum_{j=3}^{+\infty} \frac{t\kappa_j}{j!} \left(i \frac{\xi}{\sqrt{t\kappa_2}}\right)^j &= 0 \quad \lim_{t \rightarrow +\infty} \phi(\xi, t) = \lim_{t \rightarrow +\infty} e^{-\frac{\xi^2}{2} + \sum_{j=3}^{+\infty} \frac{t\kappa_j}{j!} \left(i \frac{\xi}{\sqrt{t\kappa_2}}\right)^j} \\ &= e^{-\frac{1}{2}\xi^2}.\end{aligned} \quad (19)$$

\square

3 Multivariate Maximum Likelihood Method

3.1 Maximum Likelihood Method: Numerical Approach

From a probability density function $f(x, V)$ with parameter $V = (\mu, \beta_+, \beta_-, \alpha_+, \alpha_-, \lambda_+, \lambda_-)$ and a sample data $x = (x_j)_{1 \leq j \leq m}$, we define the likelihood function, and its first and second derivatives as follows:

$$\begin{aligned} L_m(x, V) &= \prod_{j=1}^m f(x_j, V), & l_m(x, V) &= \sum_{j=1}^m \log(f(x_j, V)) \\ \frac{dl_m(x, V)}{dV_j} &= \sum_{i=1}^m \frac{df(x_i, V)}{dV_j} f(x_i, V) \\ \frac{d^2 l_m(x, V)}{dV_k dV_j} &= \sum_{i=1}^m \left(\frac{d^2 f(x_i, V)}{dV_k dV_j} \frac{df(x_i, V)}{f(x_i, V)} - \frac{df(x_i, V)}{dV_k} \frac{df(x_i, V)}{dV_j} \frac{df(x_i, V)}{f(x_i, V)} \right). \end{aligned} \quad (20)$$

To perform the maximum of the likelihood function ($L_m(x, V)$), we need the gradient of the likelihood function ($\frac{dl_m(x, V)}{dV}$) also known as the score function, and the Hessian matrix ($\frac{d^2 l_m(x, V)}{dV dV'}$), which is the variance-covariance matrix generated by the likelihood function.

Given the parameters $V = (\mu, \beta_+, \beta_-, \alpha_+, \alpha_-, \lambda_+, \lambda_-)$ and the sample data set X , we have the following quantities (21) from the previous development:

$$I'_m(X, V) = \left(\frac{dl_m(x, V)}{dV_j} \right)_{1 \leq j \leq p}, \quad I''_m(X, V) = \left(\frac{d^2 l_m(x, V)}{dV_k dV_j} \right)_{\substack{1 \leq k \leq p \\ 1 \leq j \leq p}}. \quad (21)$$

We use a computational algorithm built as a composite of a standard FRFT to compute the likelihood function and its derivatives (20) in the optimization process. More details on applying the composite of FRFTs for parameter estimations are provided in [11, 24–26]; for other computations (such probability density and cumulative functions), see [19, 27–30].

The computational algorithm yields a local solution, V , and a negative semi-definite matrix, $I''_m(x, V)$, when the following two conditions are satisfied:

$$I'_m(x, V) = 0, \quad U^T I''_m(\mathbf{X}, \mathbf{V}) U \leq 0, \quad \forall U \in \mathbb{R}^p. \quad (22)$$

The solutions, V , in (22) are provided by the Newton-Raphson iteration algorithm formula (23):

$$V^{n+1} = V^n - (I''_m(x, V^n))^{-1} I'_m(x, V^n). \quad (23)$$

More detail on maximum likelihood and Newton-Raphson iteration procedure are provided in [31].

3.2 Asymptotic Distribution of the Maximum Likelihood Estimator (MLE)

Theorem 6. (*Cramer-Rao*)

Let $T = T(X_1, \dots, X_m)$ be a statistic and write $E[T] = k(\theta)$. Then, under suitable (smoothness) assumptions,

$$\text{Var}[T] \geq \frac{\left(\frac{dE[T]}{d\theta}\right)^2}{mI(\theta)}. \quad (24)$$

For the proof of Theorem 6 refer to [32, 33].

Theorem 7. (*Consistency Estimator*)

Let X_1, \dots, X_m be independent and identically distributed (i.i.d) random variables with density $f(x|\theta)$ satisfying some regularity conditions [34]. Let θ be the true parameter, then there exists a sequence $\hat{\theta}_m = \theta_m(X_1, \dots, X_m)$ of local maxima of the likelihood function $L_m(\theta)$ which is consistent, that is, which satisfies

$$\hat{\theta}_m \xrightarrow{\text{a.s.}} \theta \quad \text{as } m \rightarrow +\infty. \quad (25)$$

More details on the proof of Theorem 7 are provided in [33, 34].

Theorem 8. (*Asymptotic Efficiency and Normality*)

Let X_1, \dots, X_m be independent and identically distributed (i.i.d) random variables with density $f(x|\theta)$ satisfying some regularity conditions in [34]. There exists a solution $\hat{\theta}_m = \theta_m(X_1, \dots, X_m)$ of the likelihood equations which is consistent, and any such solution satisfies:

$$\hat{\theta}_m - \theta \xrightarrow{d} N(0, I_m^{-1}(\theta)) \quad \text{as } m \rightarrow +\infty, \quad (26)$$

where $\theta = (\theta_1, \dots, \theta_k)$ is the actual parameter and $I_m(\theta)$ is the Fisher information matrix.

More details on the proof of Theorem 8 are provided in [34-36].

Theorem 9. (*Likelihood Ratio Test*)

Suppose the assumptions of Theorem 8 hold and that $(\hat{\theta}_{1n}, \dots, \hat{\theta}_{kn})$ are consistent roots of the likelihood equations for $\theta = (\theta_1, \dots, \theta_k)$. In addition, suppose that the corresponding assumptions hold for the parameter vector $(\theta_{r+1}, \dots, \theta_k)$ when $r < k$, and that $\hat{\theta}_{r+1,n}, \dots, \hat{\theta}_{kn}$ are consistent roots of the likelihood equations for $(\theta_{r+1}, \dots, \theta_k)$

under null hypothesis. We consider the likelihood ratio statistic

$$\frac{l_m(x, \hat{\theta})}{l_m(x, \hat{\theta})} \quad (27)$$

where $\hat{\theta} = (\theta_1, \dots, \theta_r, \hat{\theta}_{r+1, n}, \dots, \hat{\theta}_{kn})$. Then under the null hypothesis H_0 , if

$$\Delta_n = l_m(x, \hat{\theta}) - l_m(x, \hat{\theta}), \quad (28)$$

the statistic $2\Delta_n$ has a limiting χ_r^2 distribution.

More details on the proof of Theorem 9 are provided in [34, 37].

3.3 Asymptotic Test and Confidence Interval

The above results allow us to construct an asymptotically efficient estimator $\hat{\theta}_m = (\hat{\theta}_{1m}, \dots, \hat{\theta}_{km})$ of $\theta = (\theta_1, \dots, \theta_k)$ such that

$$(\hat{\theta}_{1m} - \theta_1, \dots, \hat{\theta}_{km} - \theta_k) \quad (29)$$

has a joint multivariate limit distribution with mean $(0, \dots, 0)$ and covariance matrix $I_m^{-1}(\theta) = (J_{ij})$. In particular, we have:

$$\hat{\theta}_{jm} - \theta_j \xrightarrow{d} N(0, J_{jj}) \quad \text{as } m \rightarrow +\infty. \quad (30)$$

One approach to constructing an asymptotically valid confidence interval for the parameters is via the asymptotic distribution of the ML estimator (27). An approximate $(1 - \frac{\alpha}{2})$ confidence interval for $\hat{\theta}_{jm}$ can be written as follows:

$$\hat{\theta}_{jm} \pm z\left(\frac{\alpha}{2}\right) * \sqrt{J_{jj}} \quad \text{as } m \rightarrow +\infty, \quad (31)$$

where $z(\frac{\alpha}{2})$ is the $\frac{\alpha}{2}$ quantile of the standard normal distribution.

3.4 Applications of the Log-likelihood Estimator to the Normal Distribution

We suppose the sample data $x = (x_j)_{1 \leq j \leq m}$ are independent observations and have a normal distribution [38] with parameter $V(\mu, \sigma^2)$, that is, $y \sim \mathcal{N}(\mu, \sigma^2)$, then the density is

$$f(y|V) = (2\pi\sigma^2)^{-\frac{1}{2}} \exp\left(-\frac{(y - \mu)^2}{2\sigma^2}\right). \quad (32)$$

The log-likelihood function in (20) becomes

$$l_m(x|V) = \sum_{j=1}^m \log(f(x_j|V)) = -\frac{m}{2} \log(2\pi\sigma^2) - \frac{1}{2\sigma^2} \sum_{j=1}^m (x_j - \mu)^2. \quad (33)$$

The first-order derivatives of the log-likelihood function with respect to μ and σ^2 in (20) becomes

$$I'_m(X, V) = \begin{pmatrix} \frac{dl_m(x, V)}{d\mu} \\ \frac{dl_m(x, V)}{d\sigma^2} \end{pmatrix} = \begin{pmatrix} \frac{1}{\sigma^2} \sum_{j=1}^m (x_j - \mu) \\ \frac{1}{2\sigma^4} \sum_{j=1}^m (x_j - \mu)^2 - \frac{m}{2\sigma^2} \end{pmatrix} \quad (34)$$

By setting $I'_m(X, V) = 0$, we have

$$\hat{\mu} = \frac{1}{m} \sum_{j=1}^m x_j \quad \hat{\sigma}^2 = \frac{1}{m} \sum_{j=1}^m (x_j - \hat{\mu})^2. \quad (35)$$

The second-order derivative of the log-likelihood function with respect to μ and σ^2 in (20) becomes

$$\begin{aligned} I''_m(X, V) &= \begin{pmatrix} \frac{d^2 l_m(x, V)}{d\mu^2} & \frac{d l_m(x, V)}{d\mu d\sigma^2} \\ \frac{d l_m(x, V)}{d\sigma^2 d\mu} & \frac{d^2 l_m(x, V)}{(d\sigma^2)^2} \end{pmatrix} \\ &= \begin{pmatrix} -\frac{m}{\sigma^2} & -\frac{\sum_{j=1}^m (x_j - \mu)}{\sigma^4} \\ -\frac{\sum_{j=1}^m (x_j - \mu)}{2\sigma^4} & -\frac{1}{\sigma^6} \sum_{j=1}^m (x_j - \mu)^2 + \frac{m}{2\sigma^4} \end{pmatrix} \end{aligned} \quad (36)$$

Refer to [33] for more details.

We have the Fisher information matrix and the inverse:

$$I_m(V) = -E(I''_m(X, V)) = \begin{pmatrix} \frac{m}{\sigma^2} & 0 \\ 0 & \frac{m}{2\sigma^4} \end{pmatrix} \quad I_m^{-1}(V) = \begin{pmatrix} \frac{\sigma^2}{m} & 0 \\ 0 & \frac{2\sigma^4}{m} \end{pmatrix}. \quad (37)$$

Corollary 10.

The limiting distribution of the MLE is given by:

$$\begin{pmatrix} \hat{\mu} \\ \hat{\sigma}^2 \end{pmatrix} \xrightarrow{d} N \left(\begin{pmatrix} \mu \\ \sigma^2 \end{pmatrix}, \begin{pmatrix} \frac{\sigma^2}{m} & 0 \\ 0 & \frac{2\sigma^4}{m} \end{pmatrix} \right), \quad \text{as } m \rightarrow +\infty. \quad (38)$$

The proof of Corollary 10 comes from Theorem 8, Equation (26).

4 Fitting Tempered Stable Distribution to Cryptocurrencies: Bitcoin BTC and Ethereum

4.1 Data Summaries

Bitcoin was the first cryptocurrency created in 2009 by Satoshi Nakamoto. The idea behind Bitcoin was to create a peer-to-peer electronic payment system that allows online payments to be sent directly from one party to another without going through a financial institution[39]. Since its inception, Bitcoin has grown in popularity and adoption and is now viewed as a viable legal tender in some countries. Bitcoin is currently used more as an investment tool, a risk-diversified tool, and less as a medium of exchange, a store of value, or a unit of account [19].

Bitcoin (BTC) and Ethereum (ETH) prices were extracted from CoinMarketCap. The period spans from April 28, 2013, to July 04, 2024, for Bitcoin, and from August 07, 2015, to July 04, 2024, for Ethereum.

The daily price dynamics are provided in Fig 1. The prices have an increasing trend, even after having major significant increases and decreases over the studied period. Fig 1a and Fig 1b show that Bitcoin outperforms Ethereum, which is the second-largest cryptocurrency by market capitalization after Bitcoin.

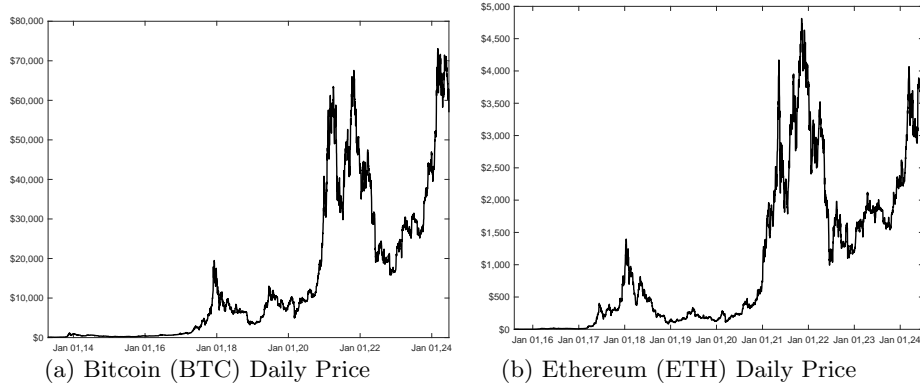


Fig. 1: Daily Price

Let m , the number of observations, and S_j , the daily observed price on the day t_j with $j = 1, \dots, m$. The daily return (y_j) is computed as follows:

$$y_j = \log(S_j/S_{j-1}) \quad j = 2, \dots, m. \quad (39)$$

As shown in Fig 2a and Fig 2b, the daily return reaches the lowest level (-46% for Bitcoin and -55% for Ethereum) in the first quarter of 2020 amid the coronavirus pandemic and massive disruptions in the global economy. Nine values were identified as outliers and removed from the data set to avoid a negative impact on the GTS model estimation and the empirical statistics.

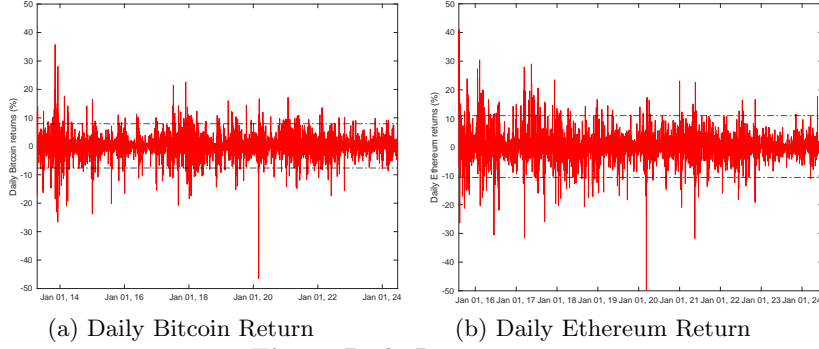


Fig. 2: Daily Return

4.2 Multidimensional Estimation Results for Cryptocurrencies

The results of the GTS parameter estimation are summarised in Table 1 for Bitcoin and Table 2 for Ethereum data. The brackets are the asymptotic standard errors computed using the inverse of the Hessian matrix built in (20). The ML estimate of μ is negative for both Bitcoin and Ethereum, while others are positive, as expected in the literature. The asymptotic standard error for μ is quite large and suggests that μ is not statistically significant at 5%.

The log-likelihood, Akaike's information Criteria (AIC), and Bayesian information criteria (BIK) statistics show that the GTS distribution with seven parameters performs better than the two-parameter Normal distribution (GBM). A comprehensive and detailed examination of the statistical significance of the results will be carried out in Section 6.

Table 1 provides a summary of the estimation results for Bitcoin returns. The skewness parameters (λ_+ , λ_-) are statistically significant at 5%.

Table 1: Maximum Likelihood GTS Parameter Estimation for Bitcoin

Model	Parameter	Estimate	Std Err	z	$Pr(Z > z)$	[95% Conf.Interval]	
GTS	μ	-0.121571	(0.375)	-0.32	7.5E-01	-0.856	0.613
	β_+	0.315548	(0.136)	2.33	2.0E-02	0.050	0.581
	β_-	0.406563	(0.117)	3.48	4.9E-04	0.178	0.635
	α_+	0.747714	(0.047)	15.76	6.2E-56	0.655	0.841
	α_-	0.544565	(0.037)	14.56	4.8E-48	0.471	0.618
	λ_+	0.246530	(0.036)	6.91	4.9E-12	0.177	0.316
	λ_-	0.174772	(0.026)	6.69	2.2E-11	0.124	0.226
	Log(ML)	-10606					
	AIC	21227					
	BIK	21271					
GBM	μ	0.151997	(0.060)	2.51	1.2E-02	0.033	0.271
	σ	3.865132	(0.330)	11.69	7.2E-32	3.217	4.513
	Log(ML)	-11313					
	AIC	22630					
	BIK	22638					

The difference is positive and statistically significant, which proves that the Bitcoin return is asymmetric and skewed to the left. The process intensity parameters (α_+ , α_-) are statistically significant at 5%. Similarly, the difference is positive and statistically significant, which shows Bitcoin is more likely to produce positive returns than negative returns. The index of stability parameters (β_+ , β_-) are both statistically significant at 5%.

However, the difference is positive but not statistically significant. The GTS distribution with $\beta = \beta_+ = \beta_-$, called Kobol distribution, was fitted as well, and the estimation results are presented in Appendix C. As shown in Table C1, all the parameters are statistically significant at 5%, and have the expected positive sign. However, the likelihood ratio test in Table 6 shows that the GTS distribution is not significantly different from the Kobol distribution as the p-value (69.6%) is large. Refer to [14] for more details on Kobol distribution

The parameters for Ethereum returns data are statistically significant at 5%, except μ and β_- . The difference ($\lambda_+ - \lambda_-$) in skewness parameters is negative and not statistically significant, showing that the Ethereum return is asymmetric and skewed to the right. Similarly, the difference ($\alpha_+ - \alpha_-$) in the intensity parameters is positive and not statistically significant, as shown the confidence interval in Table 2. Contrary to the Bitcoin return, the Ethereum return has a larger process intensity, which provides evidence that Ethereum has a lower level of peakedness and a higher level of thickness.

Table 2: Maximum Likelihood GTS Parameter Estimation for Ethereum

Model	Param	Estimate	Std Err	z	$Pr(Z > z)$	[95% Conf.Interval]	
GTS	μ	-0.4854	(1.008)	-0.48	6.3E-01	-2.461	1.491
	β_+	0.3904	(0.164)	2.38	1.7E-02	0.069	0.712
	β_-	0.4045	(0.210)	1.93	5.4E-02	-0.007	0.816
	α_+	0.9582	(0.106)	9.01	1.1E-19	0.750	1.167
	α_-	0.8005	(0.110)	7.25	4.2E-13	0.584	1.017
	λ_+	0.1667	(0.029)	5.72	1.1E-08	0.110	0.224
	λ_-	0.1708	(0.036)	4.71	2.5E-06	0.110	0.242
		Log(ML)	-9552				
	AIC	19119					
	BIK	19162					
GBM	μ	0.267284	(0.091)	2.93	3.4E-03	0.088	0.446
	σ	5.205539	(0.672)	7.74	1.0E-14	3.887	6.524
		Log(ML)	-9960				
		AIC	19925				
	BIK	19933					

We consider the following constraints $\alpha = \alpha_+ = \alpha_-$ and $\beta = \beta_+ = \beta_-$, which is the Carr–Geman–Madan–Yor (CGMY) distribution, also called Classical Tempered Stable Distribution. The CGMY distribution was fitted as well, and the estimation results are presented in Appendix D. As shown in Table D1, all the parameters are statistically significant at 5%, and have the expected positive sign. However, the likelihood ratio test in Table 6 shows, with a high p-value (35.3%), That the GTS distribution is not significantly different from the CGMY distribution, and the null

hypothesis can not be rejected. Refer to [3, 40] for more details on CGMY distribution

Table 1 and Table 2 summarized the last row of Table A1 and Table A2 respectively in appendix A, which describe the convergence process of the GTS parameter for Bitcoin and Ethereum data. The convergence process was obtained using the Newton-Raphson iteration algorithm (23). Each row has eleven columns made of the iteration number, the seven parameters μ , β_+ , β_- , α_+ , α_- , λ_+ , λ_- , and three statistical indicators: the log-likelihood ($Log(ML)$), the norm of the partial derivatives ($\|\frac{dLog(ML)}{dV}\|$), and the maximum value of the eigenvalues ($MaxEigenValue$). The statistical indicators aim at checking if the two necessary and sufficient conditions described in (22) are all met. $Log(ML)$ displays the value of the Naperian logarithm of the likelihood function $L(x, V)$, as described in (20); $\|\frac{dLog(ML)}{dV}\|$ displays the value of the norm of the first derivatives ($\frac{dL(x, V)}{dV_j}$) described in (21); and $MaxEigenValue$ displays the maximum value of the seven eigenvalues generated by the Hessian matrix ($\frac{d^2L(x, V)}{dV_k dV_j}$), as described in (21).

Similarly, Table C2 and Table D2 describe the Convergence process of the Kobl distribution parameter for Bitcoin returns and the CGMY distribution parameter for Ethereum returns.

GTS parameter estimation in Table 1 and Table 2 are used to evaluate the impact of each parameter on the GTS probability density function. As shown in Fig 3 and Fig 4, the effect of the GTS parameters on the probability density function has the same patterns on Bitcoin and Ethereum returns. However, the magnitudes are different. As shown in Fig 3a and Fig 3b, β_- (α_-) has a higher effect on the probability density function (pdf) than β_+ (α_+). However, λ_- and λ_+ in both graphs seem symmetric and have the same impact.

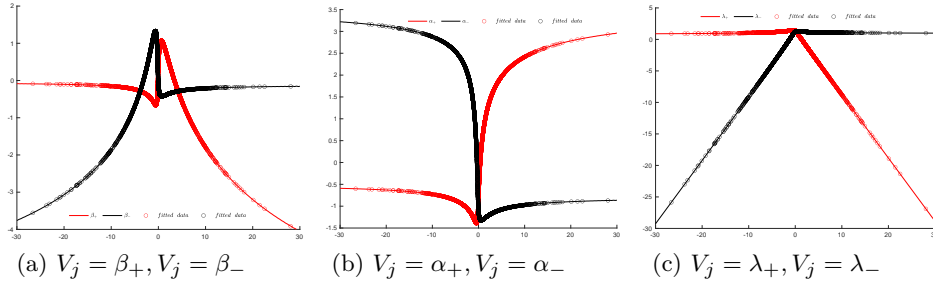


Fig. 3: $\frac{df(x, V)}{dV_j}$: Effect of parameters on the GTS probability density (Bitcoin Returns)

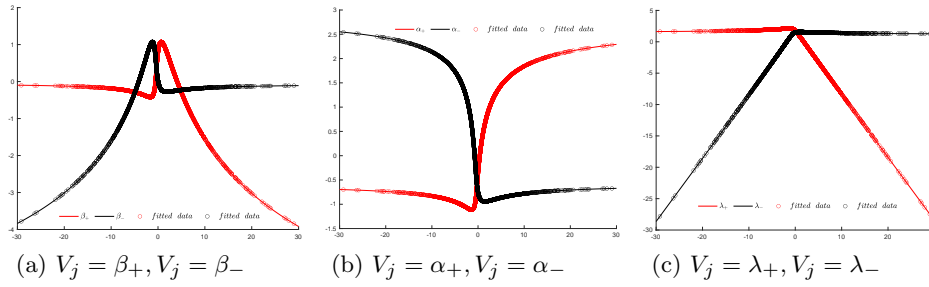


Fig. 4: $\frac{df(x,V)}{f(x,V)dV_j}$: Effect of parameters on the GTS probability density (Ethereum Returns)

4.3 Evaluation of the Method of Moments

The Method of Moments estimates the parameters of the GTS distribution by equating empirical moments and the theoretical moments of the GTS distribution. We empirically estimate the k^{th} moments ($m_k = E(x^k)$), based on sample data $x = (x_j)_{1 \leq j \leq m}$ as follows:

$$\hat{m}_k = \frac{1}{M} \sum_{j=1}^m x_j^k \quad \text{for } k = 1, \dots, 7. \quad (40)$$

On the other side, the Cumulants (κ_k) in theorem 5 can be related to the moment of the GTS distribution by the following relationship [41–43]:

$$m_k = E(x^k) = \sum_{j=1}^{k-1} \binom{k-1}{j-1} \kappa_j m_{k-j} + \kappa_k \quad \text{for } k = 1, \dots, 7. \quad (41)$$

The method of moments estimator for $V = (\mu, \beta_+, \beta_-, \alpha_+, \alpha_-, \lambda_+, \lambda_-)$ is defined as the solution to the following system of equations:

$$\hat{m}_k = m_k \quad \text{for } k = 1, \dots, 7. \quad (42)$$

The system of equations (42) is often not analytically solvable. For the conditions of existence and uniqueness of the solution, refer to [9].

Maximum likelihood GTS parameter estimation in Table 1 and Table 2 are used to evaluate the system of equations in (42). As shown in Table 3, the solution of the maximum Likelihood method satisfies at a certain extent the equations for the first four moments: $\hat{m}_1, \hat{m}_2, \hat{m}_3, \hat{m}_4$ in the system (42). The 7th moment equation has the highest relative error: 89.9% for the Bitcoin BTC and 68.3% for the Ethereum. Therefore, the maximum likelihood GTS parameter estimation is not the same as the GTS parameter estimation from the method of moments.

In addition to the method of moments estimations, the lower relative errors in Table 3 show that empirical and theoretical standard deviation (σ), skewness, and kurtosis seem to be consistent for Bitcoin and Ethereum. The empirical & theoretical statistics

show that the average Ethereum daily return is greater and more volatile than the Bitcoin daily returns. Both assets are thicker than the Normal distribution. However, the daily return of Bitcoin is skewed to the left, whereas the daily return of Ethereum is skewed to the right.

Table 3: Evaluation of the Method of Moments

	Bitcoin BTC			Ethereum		
	Empirical(1)	Theoretical(2)	$\frac{(1)-(2)}{2}$	Empirical(1)	Theoretical(2)	$\frac{(1)-(2)}{2}$
Sample size	4083			3246		
\hat{m}_1	0.152	0.152	0.0%	0.267	0.267	0.0%
\hat{m}_2	14.960	15.020	0.4%	27.161	27.388	0.8%
\hat{m}_3	-11.320	-15.640	27.6%	55.363	57.867	4.3%
\hat{m}_4	2033	2256	9.8%	5267	6307	16.5%
\hat{m}_5	-5823	-15480	62.3%	22368	32518	31.2%
\hat{m}_6	670695	1123215	40.2%	2114788	4361562	51.5%
\hat{m}_7	-1997196	-19777988	89.9%	12411809	39253001	68.3%
Standard deviation ¹	3.865	3.873	0.2%	5.206	5.226	0.4%
Skewness ²	-0.314	-0.387	18.8%	0.238	0.252	5.2%
Kurtosis ³	9.154	10.082	9.2%	7.112	8.385	15.2%
Max value	28.052			29.013		
Min Value	-26.620			-29.174		

¹ $\sigma = \sqrt{\kappa_2}$

²Skewness is estimated as $\frac{\kappa_3}{\kappa_2^{3/2}}$

³Kurtosis is estimated as $3 + \frac{\kappa_4}{\kappa_2^2}$; κ_1 , κ_2 and κ_3 are defined in (5)

5 Fitting Tempered Stable Distribution to Traditional Indices: S&P 500 and SPY ETF

5.1 Data Summaries

The Standard & Poor's 500 Composite Stock Price Index, also known as the S&P 500, is a stock index that tracks the share prices of 500 of the largest public companies with stocks listed on the New York Stock Exchange (NYSE) and the Nasdaq in the United States. It was introduced in 1957 and often treated as a proxy for describing the overall health of the stock market or the United States (US) economy. The SPDR S&P 500 ETF (SPY), also known as the SPY ETF, is an Exchange-Traded Fund (ETF) that tracks the performance of the S&P 500. SPY ETF provides a mutual fund's diversification, the stock's flexibility, and lower trading fees. The data were extracted from Yahoo Finance. The historical prices span from 04 January 2010 to 22 July 2024 and were adjusted for splits and dividends.

The daily price dynamics are provided in Fig 5. Prices have an increasing trend, even after being temporally disrupted in the first quarter of 2020 by the coronavirus pandemic. The S&P 500 is priced in thousands of US dollars, whereas the SPY ETF is in hundreds of US dollars. The SPY ETF is cheaper and provides all the attributes of the S&P 500 index, as shown in Fig 5a and Fig 5b.

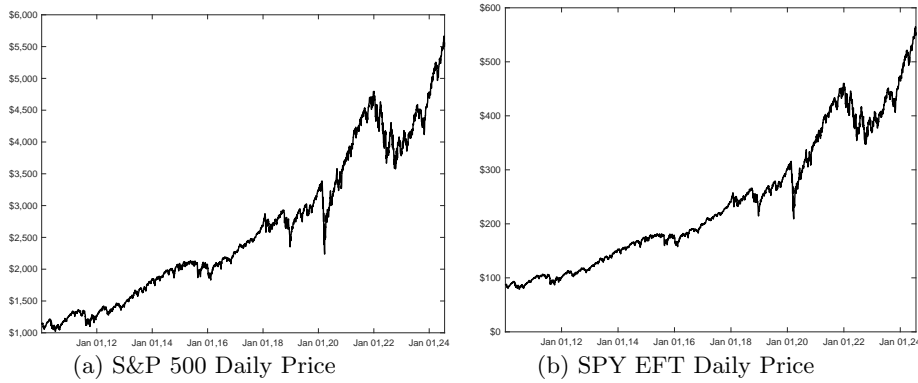


Fig. 5: Daily Price

Let the number of observations m , and the daily observed price S_j on day t_j with $j = 1, \dots, m$; t_1 is the first observation date (January 04, 2010) and t_m is the last observation date (July 22, 2024). The daily return, y_j , is computed as in (43):

$$y_j = \log(S_j/S_{j-1}) \quad j = 2, \dots, m. \quad (43)$$

SPY ETF aims to mirror the performance of the S&P 500. Fig 6a and Fig 6b look similar, which is consistent with the goal of SPY ETF. As shown in Fig 6a and Fig

6b, the daily return reaches the lowest level (-12.7% for S&P 500 and -11.5% for SPY ETF) in the first quarter of 2020 amid the coronavirus pandemic and massive disruptions in the global economy. Nine values were identified as outliers and removed from the data set to avoid a negative impact on the GTS model estimation and the empirical statistics.

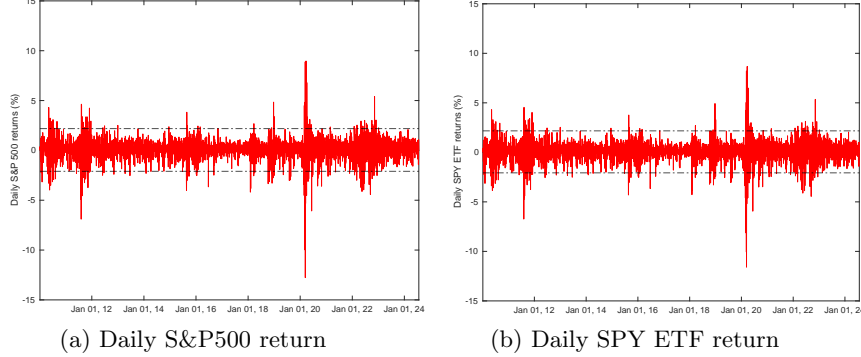


Fig. 6: Daily Return

5.2 Multidimensional Estimation Results for Traditional Indices

The estimation results are provided in Table 4 for S&P 500 return data and Table 5 for SPY EFT return data. As previously, the log-likelihood, AIC, and BIK statistics suggest that the GTS distribution with seven parameters performs better than the two-parameter Normal distribution (GBM).

As shown in both Tables 4 & 5, the ML estimate of μ is negative, while others are positive, as expected in the literature. The asymptotic standard error for μ , β_+ and β_- are pretty large and it results that μ , β_+ and β_- are not significantly different from zero.

Table 4: Maximum Likelihood GTS Parameter Estimation for S&P 500 Index

Model	Param	Estimate	Std Err	z	$Pr(Z > z)$	[95% Conf.Interval]	
GTS	μ	-0.249408	(0.208)	-1.20	2.3E-01	-0.658	0.159
	β_+	0.328624	(0.308)	1.07	2.9E-01	-0.275	0.932
	β_-	0.088640	(0.176)	0.50	6.1E-01	-0.256	0.433
	α_+	0.792426	(0.350)	2.26	2.4E-02	0.106	1.479
	α_-	0.542250	(0.107)	5.09	3.6E-07	0.333	0.751
	λ_+	1.279743	(0.348)	3.68	2.4E-04	0.597	1.962
	λ_-	0.937133	(0.144)	6.50	8.0E-11	0.655	1.220
	Log(ML)	-4920					
	AIC	9851					
	BIK	9898					
GBM	μ	0.044875	(0.018)	2.51	1.2E-02	0.010	0.080
	σ	1.081676	(0.027)	39.53	0.000	1.028	1.135
	Log(ML)	-5330					
	AIC	10665					
	BIK	10677					

However, other parameters have larger t-statistics ($|z| > 2$) and are statistically significant at 5%. Except for the index of stability parameters (β_+ , β_-), the estimation results for S&P 500 and SPY ETF indexes show that the difference in skewness parameters (λ_+ , λ_-) and intensity parameters (α_+ , α_-) are positive but are not statistically significant.

Table 5: Maximum Likelihood GTS Parameter Estimation for SPY EFT Data

Model	Param	Estimate	Std Err	z	$Pr(Z > z)$	[95% Conf.Interval]		
GTS	μ	-0.260643	(0.135)	-1.94	5.3E-02	-0.524	0.003	
	β_+	0.340880	(0.189)	1.80	7.1E-02	-0.030	0.711	
	β_-	0.022212	(0.212)	0.10	9.2E-01	-0.393	0.437	
	α_+	0.787757	(0.225)	3.50	4.6E-04	0.347	1.229	
	α_-	0.597110	(0.141)	4.22	2.4E-05	0.320	0.874	
	λ_+	1.288555	(0.226)	5.70	1.2E-08	0.846	1.731	
	λ_-	1.014353	(0.177)	5.74	9.4E-09	0.668	1.361	
		Log(ML)	-4893					
	AIC	9800						
	BIK	9843						
GBM	μ	0.054344	(0.017)	3.13	1.8E-03	0.020	0.088	
	σ	1.050217	(0.026)	40.71	0.000	1.000	1.101	
		Log(ML)	-54275					
		AIC	10554					
		BIK	10566					

The hypothesis with $\beta_+ = \beta_- = 0$ was considered by fitting the S&P 500 and SPY ETF indexes to the Bilateral Gamma distribution. The estimation results are summarised in Appendix E & F. As shown in Table E1 and Table F1, the skewness parameters (λ_+ , λ_-) are positive and statistically significant, and the difference ($\lambda_+ - \lambda_-$) is also positive and statistically significant, which prove that S&P 500 and SPY ETF returns are skewed to the left. We have the same statistical features for the intensity parameters (α_+ , α_-), and Both indexes are more likely to produce positive returns than negative returns. Refer to [44, 45] for more details on Bilateral Gamma distribution.

The likelihood ratio test in Table 6 shows that, even with non-statistically significant parameters, the GTS distribution fits significantly better than the Bilateral Gamma distribution for both S&P 500 and SPY ETF indexes. Contrary to the AIC statistics, the BIK statistics do not provide the same information. A comprehensive and detailed examination of the statistical significance of the results is carried out in Section 6.

Table 4 and Table 5 summarized the last row of Table A3 and Table A4, respectively in appendix A, which describe the convergence process of the GTS parameter for Bitcoin, Ethereum, S&P 500 index and SPY ETF return data. The convergence process was obtained using the Newton-Raphson iteration algorithm (23). Each row has eleven columns made of the iteration number, the seven parameters μ , β_+ , β_- , α_+ , α_- , λ_+ , λ_- , and three statistical indicators: the log-likelihood ($Log(ML)$), the norm

of the partial derivatives ($\|\frac{dLog(ML)}{dV}\|$), and the maximum value of the eigenvalues ($MaxEigenValue$). The statistical indicators aim at checking if the two necessary and sufficient conditions described in (22) are all met. $Log(ML)$ displays the value of the Naperian logarithm of the likelihood function $L(x, V)$, as described in (20); $\|\frac{dLog(ML)}{dV}\|$ displays the value of the norm of the first derivatives ($\frac{dl(x,V)}{dV_j}$) described in Equation (21); and $MaxEigenValue$ displays the maximum value of the seven eigenvalues generated by the Hessian matrix ($\frac{d^2l(x,V)}{dV_k dV_j}$), as described in (21).

Similarly, Table E2 and Table F2 describe the convergence process of the Bilateral Gamma distribution parameter for S&P 500 index and SPY ETF return data.

Table 6: Likelihood Ratio Test Statistic & P-value

		GTS	GTS variants	χ^2 -Value	df	P-Value
Bitcoin	Log(ML)	-10606.73	-10606.81	0.1525	1	0.6962
	AIC	21227.47	21225.62			
	BIK	21271.67	21263.51			
Ethereum	Log(ML)	-9552.86	-9553.90	2.0810	2	0.3533
	AIC	19119.72	19117.81			
	BIK	19162.32	19148.23			
S&P 500	Log(ML)	-4920.52	-4924.62	8.1828	2	0.0167
	AIC	9851.06	9859.24			
	BIK	9898.49	9890.26			
SPY ETF	Log(ML)	-4893.21	-4898.67	10.9234	2	0.0042
	AIC	9800.42	9807.34			
	BIK	9843.84	9838.36			

GTS parameter estimation in Table 4 and Table 5 were used to evaluate the impact of the parameters on the GTS probability density function. As shown in Fig 7 and Fig 8, the effect of the GTS parameters on the probability density function generated by S&P 500 and SPY ETF have the same patterns. As shown in Fig 7a and Fig 7b, based on the S&P 500 return data, β_+ (α_+) has a higher effect on the probability density function than β_- (α_-). However, λ_- and λ_+ in Fig 7c are symmetric and have the same impact.

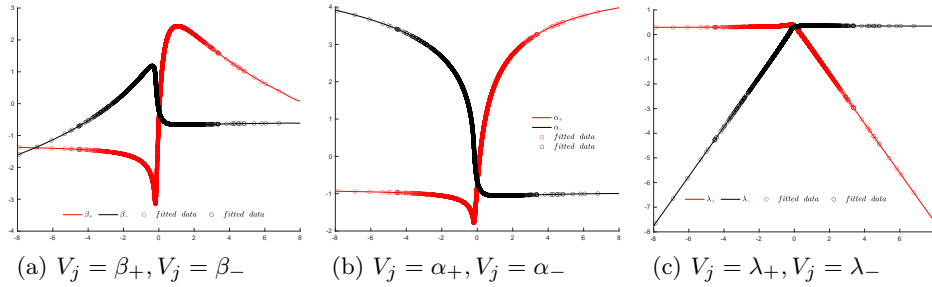


Fig. 7: $\frac{df(x,V)}{dV_j}$: Effect of Parameters on the GTS Probability Density (S&P 500 Index)

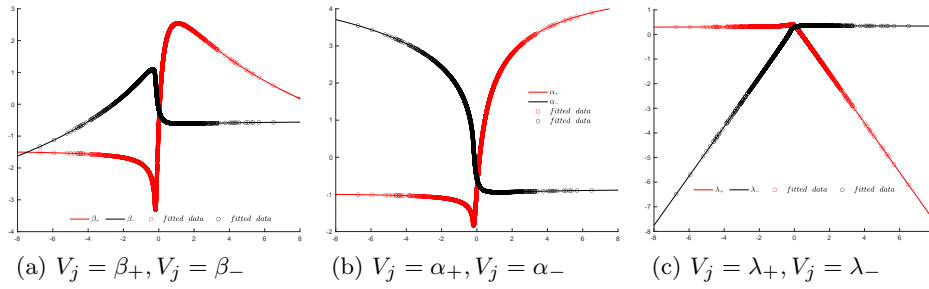


Fig. 8: $\frac{df(x, V)}{dV_j}$: Effect of Parameters on the GTS Probability Density (SPY EFT)

5.3 Evaluation of the Methods of Moments

Maximum likelihood GTS parameter estimation in Table 4 and Table 5 are used to evaluate the system of equations in (42). As shown in Table 7, the solution of the maximum likelihood method satisfies at a certain extent the equations for the following four moments: \hat{m}_1 , \hat{m}_2 , \hat{m}_4 , \hat{m}_5 in the system (42). As for Bitcoin and Ethereum, the 7th moment equation has the highest relative error: 53.3% for S&P 500 index and -85.9% for SPY ETF. Therefore, the maximum likelihood GTS parameter estimation is not the GTS parameter estimation from the method of moments.

Table 7: Evaluation of the Methods of Moment

	S&P 500 Index			SPY ETF		
	Empirical(1)	Theoretical(2)	$\frac{(1)-(2)}{2}$	Empirical(1)	Theoretical(2)	$\frac{(1)-(2)}{2}$
Sample size	3656			3655		
\hat{m}_1	0.045	0.045	-0.5%	0.054	0.054	0.0%
\hat{m}_2	1.069	1.083	-1.3%	1.053	1.044	0.8%
\hat{m}_3	-0.447	-0.341	31.2%	-0.214	-0.351	-39.0%
\hat{m}_4	8.371	9.764	-14.3%	8.197	7.691	6.6%
\hat{m}_5	-16.386	-11.128	47.3%	-3.969	-12.717	-68.8%
\hat{m}_6	193.563	247.811	-21.9%	157.645	162.048	-2.7%
\hat{m}_7	-840.097	-547.882	53.3%	-85.003	-602.447	-85.9%
Standard deviation ¹	1.082	1.033	4.7%	1.050	1.021	2.9%
Skewness ²	-0.432	-0.535	-19.2%	-0.358	-0.490	-26.9%
Kurtosis ³	8.413	7.435	13.1%	7.495	7.177	4.4%
Max value	6.797			6.501		
Min Value	-7.901			-6.734		

In addition to the moment estimations in Table 7, the lower relative errors show that the empirical and theoretical standard deviation (σ), skewness, and kurtosis are consistent for S&P 500 and SPY ETF. The empirical & theoretical statistics show that both assets are skewed to the left and also thicker than the Normal distribution.

¹ $\sigma = \sqrt{\kappa_2}$

² Skewness is estimated as $\frac{\kappa_3}{3/2}$

³ Kurtosis is estimated as $3 + \frac{\kappa_4}{\kappa_2^2}$; κ_1 , κ_2 and κ_3 are defined in (5)

6 Goodness-of-fit Analysis

6.1 Kolmogorov-Smirnov (KS) Analysis

Given the sample of daily return $\{y_1, y_2 \dots y_m\}$ of size m and the empirical cumulative distribution function, $F_m(x)$, for each index, the Kolmogorov-Smirnov (KS) test is performed under the null hypothesis, H_0 , that the sample $\{y_1, y_2 \dots y_m\}$ comes from the GTS distribution, $F(x)$. The cumulative distribution function of the theoretical distribution, $F(x)$, needs to be computed. The density function, $f(x)$, does not have a closed form, the same for the cumulative function, $F(x)$, in (45). However, we know the closed form of the Fourier of the density function, $\mathcal{F}[f]$, and the relationship in (46) provides the Fourier of the cumulative distribution function, $\mathcal{F}[F]$. The GTS distribution function, $F(x)$, was computed from the inverse of the Fourier of the cumulative distribution, $\mathcal{F}[F]$, in (47):

$$Y \sim GTS(\mu, \beta_+, \beta_-, \alpha_+, \alpha_-, \lambda_+, f\lambda_-) \quad (44)$$

$$F(x) = \int_{-\infty}^x f(t)dt \quad f \text{ is the density function of } Y \quad (45)$$

$$\mathcal{F}[F](x) = \frac{\mathcal{F}[f](x)}{ix} + \pi \mathcal{F}[f](0)\delta(x) \quad (46)$$

$$F(x) = \frac{1}{2\pi} \int_{-\infty}^{+\infty} \frac{\mathcal{F}[f](y)}{iy} e^{ixy} dy + \frac{1}{2} \quad (47)$$

See Appendix A in [45] for (46) proof.

The two-sided KS goodness-of-fit statistic (D_m) is defined as follows:

$$D_m = \sup_x |F(x) - F_m(x)|, \quad (48)$$

where m is the sample size, $F_m(x)$ denotes the empirical cumulative distribution of $\{y_1, y_2 \dots y_m\}$.

The distribution of Kolmogorov's goodness-of-fit measure D_m has been studied extensively in the literature. It was shown [46] that the D_m distribution is independent of the theoretical distribution, $F(x)$, under the null hypothesis, H_0 . The discrete, mixed, and discontinuous distributions case has also been studied [47]. Under the null hypothesis, H_0 , that the sample $\{y_1, y_2 \dots y_m\}$ of size m comes from the hypothesized continuous distribution, it was shown [48] that the asymptotic statistic $\sqrt{n}D_n$ converges to the Kolmogorov distribution.

The limiting form for the distribution function of Kolmogorov's goodness-of-fit measure D_m is

$$\lim_{m \rightarrow +\infty} Pr(\sqrt{m}D_m \leq x) = 1 - 2 \sum_{k=1}^{+\infty} (-1)^{k-1} e^{-2k^2 x^2} = \frac{\sqrt{2\pi}}{x} \sum_{k=1}^{+\infty} e^{-\frac{(2k-1)^2 \pi^2}{8x^2}}. \quad (49)$$

The first representation was given in [48], and the second came from a standard relation for theta functions [49].

As shown in Fig 9, the asymptotic statistic, $\sqrt{n}D_n$, is a positively skewed distribution with a mean and a standard deviation [49]

$$\mu = \sqrt{\frac{\pi}{2}} \log(2) \sim 0.8687, \quad \sigma = \sqrt{\frac{\pi^2}{12} - \mu^2} \sim 0.2603. \quad (50)$$

At 5% risk level, the risk threshold is $d = 1.3581$ and represents the area in the shaded area under the probability density function.

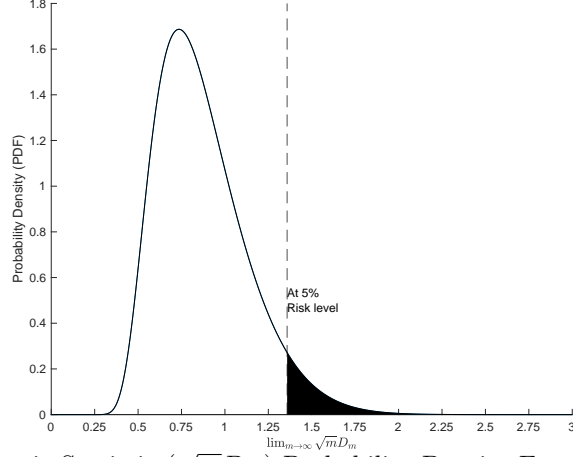


Fig. 9: Asymptotic Statistic ($\sqrt{m}D_m$) Probability Density Function (PDF)

The p-value of the test statistic, D_m , is computed based on (49) as follows:

$$P_value = Pr(D_m > \hat{D}_m | H_0) = 1 - Pr(\sqrt{m}D_m \leq \sqrt{m}\hat{D}_m). \quad (51)$$

A p-value is defined as the probability that values are even more extreme or more in the tail than our test statistic. A small p-value leads to a rejection of the null hypothesis, H_0 , because the test statistic, D_m , is already extreme. We reject the hypothesis if the p-value is less than our level of significance, which we take to be equal to 0.05.

\hat{D}_m is a realization value of the KS estimator D_m computed from the sample $\{y_1, y_2 \dots y_m\}$. \hat{D}_m is estimated [50] as follows:

$$\hat{D}_m = \text{Max} \left(\sup_{0 \leq j \leq P} |F(x_j) - F_m(x_j)|, \sup_{1 \leq j \leq P} |F(x_j) - F_m(x_{j-1})| \right). \quad (52)$$

The following computations were performed for Bitcoin BTC data, and the quantity \hat{D}_m was obtained:

$$\begin{aligned}
\sup_{0 \leq j \leq P} |F(x_j) - F_m(x_j)| &= 0.01300 \\
\sup_{1 \leq j \leq P} |F(x_j) - F_m(x_{j-1})| &= 0.00538 \\
\hat{D}_m &= 0.01300 \\
P_value &= \text{prob}(\sqrt{m}D_m > 0.6903 | H_0) = 49.48\%.
\end{aligned} \tag{53}$$

For each index and model, KS-statistics (\hat{D}_m) and p-values associated were computed and summarized in Table 8 along with the index sample size, m .

Table 8: Kolmogorov-Smirnov Statistic & P-value

Index	GTS			GBN			GTS variants			Sample size m
	\hat{D}_m	$\sqrt{m}\hat{D}_m$	P_value	\hat{D}_m	$\sqrt{m}\hat{D}_m$	P_value	\hat{D}_m	$\sqrt{m}\hat{D}_m$	P_value	
Bicoin BTC	0.013	0.830	0.494	0.106	6.803	0.000	0.014 ⁴	0.863	0.445	4083
Ethereum	0.012	0.721	0.674	0.092	5.249	0.000	0.013 ⁵	0.749	0.627	3246
S&P 500	0.012	0.750	0.627	0.091	5.550	0.000	0.014 ⁶	0.897	0.395	3656
SPY ETF	0.014	0.869	0.436	0.089	5.438	0.000	0.016 ⁶	1.010	0.258	3655

The asymptotic statistics, $\sqrt{n}D_n$, produced from the two-parameter geometric Brownian motion (GBM) hypothesis, have high values and show that the GBM hypothesis is always rejected. On the other hand, the high p-values generated by the asymptotic statistics suggest insufficient evidence to reject the assumption that the data were randomly sampled from a GTS. The same observations work for the GTS variants: Kobl, CGMY, and Bilateral Gamma distributions. In addition, as shown the p-value indicator in Table 8, the GTS distribution outperforms the Bilateral Gamma distribution for the S&P 500 and SPY ETF indexes. However, the Kobl and CGMY distributions respectively, for Bitcoin and Ethereum have almost the same performance as the GTS distribution.

6.2 Anderson-Darling Test Analysis

The Anderson-Darling test [51] is a goodness-of-fit test that allows the control of the hypothesis that the distribution of a random variable observed in a sample follows a certain theoretical distribution. The Anderson-Darling statistic belongs to the class of quadratic EDF statistics[52] based on the empirical distribution function. The quadratic EDF statistics measure the distance between the hypothesized distribution

⁴Kobl distribution ($\beta = \beta_- = \beta_+$)

⁵Carr-Geman-Madan-Yor (CGMY) distributions ($\beta = \beta_- = \beta_+$; $\alpha = \alpha_- = \alpha_+$)

⁶bilateral Gamma distribution ($\beta_- = \beta_+ = 0$)

$(F(x))$ and empirical distribution. It is defined as

$$m \int_{-\infty}^{+\infty} (F_m(x) - F(x))^2 w(x) dF(x), \quad (54)$$

where m is the number of elements in the sample, $w(x)$ is a weighting function, and $F_n(x)$ is the empirical distribution function defined on the sample of size n .

When the weighting function is $w(x) = 1$, the statistic (54) is the Cramér–von Mises statistic, while the Anderson–Darling statistic is obtained by choosing the weighting function $w(x) = F(x)(1 - F(x))$. Compared with the Cramér–von Mises statistic, the Anderson–Darling statistic places more weight on the tails of the distribution.

The Anderson–Darling statistic is

$$A_m^2 = m \int_{-\infty}^{+\infty} \frac{(F_m(x) - F(x))}{F(x)(1 - F(x))} dF(x). \quad (55)$$

It can be shown that the asymptotic distribution of the Anderson–Darling statistic, A_m^2 , is independent of the theoretical distribution under the null hypothesis. The asymptotic distribution [53, 54] is defined as follows:

$$\begin{aligned} G(x) &= \lim_{m \rightarrow \infty} Pr [A_m^2 < x] = \sum_{j=0}^{+\infty} a_j (xb_j)^{-\frac{1}{2}} \exp\left(-\frac{b_j}{x}\right) \int_0^{+\infty} f_j(y) \exp(-y^2) dy \\ f_j(y) &= \exp\left(\frac{1}{8} \frac{xb_j}{y^2x + b_j}\right), \quad a_j = \frac{(-1)^j (2)^{\frac{1}{2}} (4j+1) \Gamma(j + \frac{1}{2})}{j!} \\ b_j &= \frac{1}{2} (4j+1)^2 \pi^2. \end{aligned} \quad (56)$$

As shown in Fig 10, the asymptotic distribution of the Anderson–Darling statistic (A_m^2) is a positively skewed distribution with a mean and a standard deviation [55]

$$\mu = 1, \quad \sigma = \sqrt{\frac{2}{3}(\pi^2 - 9)} \sim 0.761. \quad (57)$$

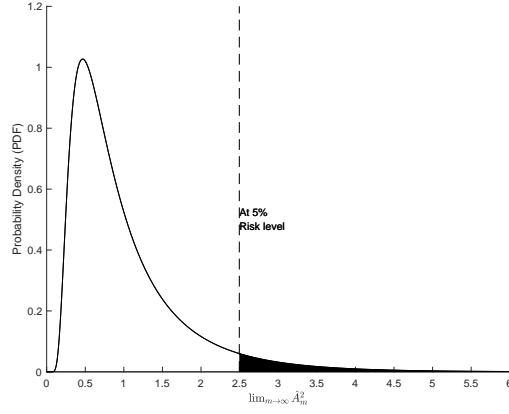


Fig. 10: Asymptotic Anderson–Darling Statistic (A_m^2) Probability Density Function (PDF)

At 5% risk level, the risk threshold is $d = 2.4941$ and represents the area in the shaded area under the probability density function.

The p-value of the test statistic, A_m^2 , is defined as follows:

$$P_value = \text{prob}(A_m^2 > \hat{A}_m^2 | H_0) = 1 - G(\hat{A}_m^2). \quad (58)$$

In order to compute the Anderson–Darling statistic, A_m^2 , in (55), the sample of daily return $\{y_1, y_2 \dots y_m\}$ of size m is arranged in ascending order: $y_{(1)} < y_{(2)} < \dots < y_{(m)}$. The Anderson–Darling statistic [53] then becomes

$$A_m^2 = -m - \frac{1}{m} \sum_{j=1}^m [(2j-1)\log(F(y_{(j)})) + (2(n-j)+1)\log(F(y_{(j)}))]. \quad (59)$$

For each index, the Anderson–Darling statistic (59) is computed along with the p-value statistic. Table 9 shows the KS-statistics (A_m^2) and P_values for the GTS, GBM, and the GTS variant distributions. While the two-parameter GBM hypothesis is always rejected, the GTS hypothesis is accepted and yields a very high p-value.

Table 9: Anderson–Darling Statistic & P-value

Index	GTS		GBN		GTS variants		Sample size
	\hat{A}_m^2	P_value	\hat{A}_m^2	P_value	\hat{A}_m^2	P_value	m
Bicoïn BTC	0.1098	0.9999	99.706	0.0000	0.1105 ⁴	0.9999	4083
Ethereum	0.1018	0.9999	59.157	0.0001	0.2123 ⁵	0.9866	3246
S&P 500	0.3007	0.9376	54.304	0.0001	0.5010 ⁶	0.7458	3656
SPY ETF	0.3017	0.9368	51.516	0.0001	0.6684 ⁶	0.5857	3655

⁴Kobol distribution ($\beta = \beta_- = \beta_+$)

⁵Carr-Geman-Madan-Yor (CGMY) distributions ($\beta = \beta_- = \beta_+$; $\alpha = \alpha_- = \alpha_+$)

⁶Bilateral Gamma distribution ($\beta_- = \beta_+ = 0$)

In addition, as shown by the p-value indicator in Table 9, the GTS distribution outperforms the Bilateral Gamma distribution for the S&P 500 and SPY ETF indexes. However, the Kobol and CGMY distributions for Bitcoin and Ethereum, respectively, have almost the same performance as the GTS distribution.

6.3 Pearson's Chi-squared Test Analysis

Pearson's chi-squared test [56] counts the number of sample points falling into certain intervals and compares them with the expected number under the null hypothesis. Under the null hypothesis, H_0 , a random sample $\{y_1, y_2 \dots y_m\}$ comes from the GTS distribution, which depends on the seven parameters estimated in Section 4. Suppose that m observations in the sample from a population are classified into K mutually exclusive classes with respective observed numbers of observations N_j (for $j = 1, 2, \dots, K$), and a null hypothesis gives the probability $\Pi_j = F(x_j) - F(x_{j-1})$ (47) that an observation falls into the j^{th} class.

The following Pearson statistic calculates the value of the chi-squared goodness-of-fit test:

$$\chi^2(K - 1 - p) = \sum_{j=1}^K \frac{(N_j - m\Pi_j)^2}{m\Pi_j}. \quad (60)$$

Under the null hypothesis assumption, as m goes to $+\infty$, the limiting distribution[56] of the Pearson statistic (60) follows the $\chi^2(K - 1 - p)$ distribution with $K - 1 - p$ degrees of freedom, p is the number of estimated parameters.

Table 10 shows the Pearson chi-squared statistics ($\hat{\chi}^2(K - 1 - p)$), P -values and Class Number for the GTS, GBM and the GTS variant distributions. While the two-parameter GBM hypothesis is always rejected, the GTS hypothesis is accepted and yields a high p-value.

Table 10: Pearson Statistics & P-values

	GTS		GBN		GTS variants			Class Number
Index	$\hat{\chi}^2(K - 8)$	P_value	$\hat{\chi}^2(K - 3)$	P_value	$\hat{\chi}^2(K - p - 1)$	p	P_value	K
Bicoin BTC	12.234	0.508	1375	0.000	12.549 ⁴	6	0.562	21
Ethereum	6.910	0.863	805	0.000	8.618 ⁵	5	0.854	20
S&P 500	9.886	0.703	574	0.000	12.844 ⁶	5	0.614	21
SPY ETF	13.955	0.377	605	0.000	18.228 ⁶	5	0.251	21

In addition, as shown by the p-value indicator in Table 10, the GTS distribution outperforms the Bilateral Gamma distribution for the S&P 500 and SPY ETF indexes. However, the Kobol and CGMY distributions for Bitcoin and Ethereum, respectively, have almost the same performance as the GTS distribution. For more details on the

⁴Kobol distribution ($\beta = \beta_- = \beta_+$)

⁵Carr-Geman-Madan-Yor (CGMY) distributions ($\beta = \beta_- = \beta_+$; $\alpha = \alpha_- = \alpha_+$)

⁶Bilateral Gamma distribution ($\beta_- = \beta_+ = 0$)

estimation of the Pearson-statistic inputs under the GTS distribution, refer to Table B1 in Appendix B.

7 Conclusion

The study provides a methodology for fitting the rich class of the seven-parameter GTS distribution to financial data. Four historical prices were considered in the methodology application: two heavily tailed data (Bitcoin and Ethereum returns) and two peaked data (S&P 500 and SPY ETF returns). In the study, each historical data was used to fit the seven-parameter GTS distribution to the underlying data return distribution. The advanced fast FRFT scheme, which is based on the classic fast FRFT algorithm and the 11-point composite Newton–Cotes rule, was used to perform the maximum likelihood estimation of seven parameters of the GTS distribution. The maximum likelihood estimate results show that, for each index, the location parameter, μ , is negative while others are positive, as expected in the literature. The statistical significance of the parameters was analyzed. The non-statistical significance of the index of stability parameters (β_+ , β_-) has led to the fitting of the Kobol, CGMY, and the Bilateral Gamma distributions. The goodness-of-fit was assessed through Kolmogorov-Smirnov, Anderson-Darling, and Pearson's chi-squared statistics. While the two-parameter GBM hypothesis is always rejected, the goodness-of-fit analysis shows that the GTS distribution fits significantly the four historical data with a very high p-value.

As a main limitation of the study, The applied methodology is compute-intensive, and the researchers need good skills in computer programming. In future work, the estimated parameter of the GTS distribution will be used in the Ornstein-Uhlenbeck type process to simulate the daily cumulative returns of the financial asset.

References

- [1] Sato, K.-I.: Lévy Processes and Infinitely Divisible Distributions. Cambridge university press, Cambridge (1999)
- [2] Nolan, J.P.: 2. Modeling with Stable Distributions, pp. 25–52. Springer, Cham (2020). https://doi.org/10.1007/978-3-030-52915-4_2
- [3] Rachev, S.T., Kim, Y.S., Bianchi, M.L., Fabozzi, F.J.: Stable and tempered stable distributions. In: S.T. Rachev, M.L.B. Y.S. Kim, Fabozzi, F.J. (eds.) Financial Models with Lévy Processes and Volatility Clustering. The Frank J. Fabozzi Series, vol. 187, pp. 57–85. John Wiley & Sons, Ltd, Hoboken, New Jersey (2011). <https://doi.org/10.1002/9781118268070>
- [4] Nzokem, A.H.: Self-decomposable laws associated with general tempered stable (gts) distribution and their simulation applications. ArXiv e-prints (2024) [arXiv:2405.16614](https://arxiv.org/abs/2405.16614) [math.PR]
- [5] Borak, S., Härdle, W., Weron, R.: Stable distributions. In: Statistical Tools for Finance and Insurance, pp. 21–44. Springer, Berlin, Heidelberg (2005). https://doi.org/10.1007/3-540-27395-6_1
- [6] Tsallis, C.: Lévy distributions. Physics World **10**(7), 42 (1997) <https://doi.org/10.1088/2058-7058/10/7/32>

- [7] Grabchak, M., Samorodnitsky, G.: Do financial returns have finite or infinite variance? a paradox and an explanation. *Quantitative Finance* **10**(8), 883–893 (2010)
- [8] Kim, Y.S., Rachev, S.T., Bianchi, M.L., Fabozzi, F.J.: A new tempered stable distribution and its application to finance. In: Georg, B., Svetlozar, T.R., Reinhold, W. (eds.) *Risk Assessment: Decisions in Banking and Finance*, pp. 77–109 (2009). Springer
- [9] K uchler, U., Tappe, S.: Tempered stable distributions and processes. *Stochastic Processes and their Applications* **123**(12), 4256–4293 (2013)
- [10] Massing, T.: Parametric estimation of tempered stable laws. *ALEA, Lat. Am. J. Probab. Math. Stat* **21**, 1567–1600 (2024) <https://doi.org/10.30757/ALEA.v21-59>
- [11] Nzokem, A.H., Montshiwa, V.T.: Fitting generalized tempered stable distribution: Fractional fourier transform (frft) approach. *ArXiv e-prints* (2022) [arXiv:2205.00586](https://arxiv.org/abs/2205.00586) [q-fin.ST]
- [12] Fallahgoul, H., Loeper, G.: Modelling tail risk with tempered stable distributions: an overview. *Annals of Operations Research* **299**, 1253–1280 (2021)
- [13] Nzokem, A.H.: Enhanced the fast fractional fourier transform (frft) scheme using the closed newton-cotes rules. *ArXiv e-prints* (2023) [arXiv:2311.16379](https://arxiv.org/abs/2311.16379) [math.NA]
- [14] Boyarchenko, S., Levendorskii, S.Z.: *Non-Gaussian Merton-Black-Scholes Theory* vol. 9. World Scientific Publishing, Singapore (2002)
- [15] Fallahgoul, H.A., Veredas, D., Fabozzi, F.J.: Quantile-based inference for tempered stable distributions. *Computational Economics* **53**, 51–83 (2019)
- [16] Bianchi, M.L., Stoyanov, S.V., Tassinari, G.L., Fabozzi, F.J., Focardi, S.M.: *Handbook of Heavy-Tailed Distributions in Asset Management and Risk Management. Financial Economics*, vol. 7. World Scientific Publishing, Singapore (2019). <https://doi.org/10.1142/11118>
- [17] Barndorff-Nielsen, O.E., Shephard, N.: Financial volatility, L evy processes and power variation. 2002. Available online: https://www.olsendata.com/data_products/client_papers/papers/200206-NielsenShephard-FinVolLevyProcessPowerVar.pdf Last accessed: 2024-08-27
- [18] Ken-Iti, S.: Basic results on l evy processes. In: Barndorff-Nielsen, O.E., Mikosch, T., Resnick, S.I. (eds.) *L evy Processes: Theory and Applications*, pp. 1–37. Springer, New York, NY (2001). <https://doi.org/10.1007/978-1-4612-0197-7>
- [19] Nzokem, A.H., Maposa, D.: Bitcoin versus s&p 500 index: Return and risk analysis. *Mathematical and Computational Applications* **29**(3) (2024) <https://doi.org/10.3390/mca29030044>
- [20] Nzokem, A.H.: Pricing european options under stochastic volatility models: Case of five-parameter variance-gamma process. *Journal of Risk and Financial Management* **16**(1) (2023) <https://doi.org/10.3390/jrfm16010055>
- [21] Madan, D.B., Carr, P.P., Chang, E.C.: The variance gamma process and option pricing. *Review of Finance* **2**(1), 79–105 (1998)
- [22] Kendall, M.G.: *The Advanced Theory of Statistics* vol. 1, 2nd edn. Charles Griffin & Co. Ltd, London (1945)

- [23] Feller, W.: An Introduction to Probability Theory and Its Applications, Volume 2 vol. 2, 2nd edn. John Wiley & Sons, New York (1971)
- [24] Nzokem, A.H.: Gamma variance model: Fractional fourier transform (FRFT). *Journal of Physics: Conference Series* **2090**(1), 012094 (2021) <https://doi.org/10.1088/1742-6596/2090/1/012094>
- [25] Nzokem, A.H., Montshiwa, V.T.: The ornstein–uhlenbeck process and variance gamma process: Parameter estimation and simulations. *Thai Journal of Mathematics*, 160–168 (2023). Accessed 2024-08-02
- [26] Nzokem, A.H.: Numerical solution of a gamma - integral equation using a higher order composite newton-cotes formulas. *Journal of Physics: Conference Series* **2084**(1), 012019 (2021) <https://doi.org/10.1088/1742-6596/2084/1/012019>
- [27] Nzokem, A.H.: European option pricing under generalized tempered stable process: Empirical analysis. *ArXiv e-prints* (2023) [arXiv:2304.06060](https://arxiv.org/abs/2304.06060) [q-fin.PR]
- [28] Eberlein, E., Glau, K., Papapantoleon, A.: Analysis of fourier transform valuation formulas and applications. *Applied Mathematical Finance* **17**(3), 211–240 (2010)
- [29] Eberlein, E.: Fourier-based valuation methods in mathematical finance. In: Benth, F.E., Kholodnyi, V.A., Laurence, P. (eds.) *Quantitative Energy Finance: Modeling, Pricing, and Hedging in Energy and Commodity Markets*, pp. 85–114. Springer, New York, NY (2014). https://doi.org/10.1007/978-1-4614-7248-3_3 . https://doi.org/10.1007/978-1-4614-7248-3_3
- [30] Cherubini, U., Della Lunga, G., Mulinacci, S., Rossi, P.: *Fourier Transform Methods in Finance*. John Wiley & Sons, ??? (2010)
- [31] Giudici, P., Givens, G.H., Mallick, B.K.: *Wiley Series in Computational Statistics*. Wiley Online Library, New Jersey (2013)
- [32] Bos, A.: 4. Precision and Accuracy, pp. 45–97. John Wiley & Sons, Ltd, ??? (2007). <https://doi.org/10.1002/9780470173862.ch4>
- [33] Casella, G., Berger, R.: *Statistical Inference*. Chapman & Hall/CRC Texts in Statistical Science. CRC Press, New York (2024). <https://books.google.com.ng/books?id=cqUIEQAAQBAJ>
- [34] Lehmann, E.L.: *Elements of Large-sample Theory*. Springer, New York (1999)
- [35] Olive, D.J.: *Statistical Theory and Inference*. Springer, New York (2014)
- [36] Hall, W.J., Oakes, D.: *A Course in the Large Sample Theory of Statistical Inference*. CRC Press, New York (2023)
- [37] Vuong, Q.H.: Likelihood ratio tests for model selection and non-nested hypotheses. *Econometrica: journal of the Econometric Society*, 307–333 (1989)
- [38] Mensah, E.T., Boateng, A., Frempong, N.K., Maposa, D.: Simulating stock prices using geometric brownian motion model under normal and convoluted distributional assumptions. *Scientific African* **19**, 01556 (2023) <https://doi.org/10.1016/j.sciaf.2023.e01556>
- [39] Nakamoto, S.: Bitcoin: A peer-to-peer electronic cash system. *Decentralized Bus. Rev.* 2008. Available online: https://www.ussc.gov/sites/default/files/pdf/training/annual-national-training-seminar/2018/Emerging_Tech_Bitcoin_Crypto.pdf (Last accessed: 2024-05-10)
- [40] Carr, P., Geman, H., Madan, D.B., Yor, M.: Stochastic volatility for lévy processes. *Mathematical finance* **13**(3), 345–382 (2003)

- [41] Smith, P.J.: A recursive formulation of the old problem of obtaining moments from cumulants and vice versa. *The American Statistician* **49**(2), 217–218 (1995). Accessed 2024-09-16
- [42] Poloskov, I.E.: Relations between cumulants and central moments and their applications. *Journal of Physics: Conference Series* **1794**(1), 012004 (2021) <https://doi.org/10.1088/1742-6596/1794/1/012004>
- [43] Rota, G.-C., Shen, J.: On the combinatorics of cumulants. *Journal of Combinatorial Theory, Series A* **91**(1), 283–304 (2000) <https://doi.org/10.1006/jcta.1999.3017>
- [44] K uchler, U., Tappe, S.: Bilateral gamma distributions and processes in financial mathematics. *Stochastic Processes and their Applications* **118**(2), 261–283 (2008) <https://doi.org/10.1016/j.spa.2007.04.006>
- [45] Nzokem, A.H.: Fitting infinitely divisible distribution: Case of gamma-variance model. *ArXiv e-prints* (2021) [arXiv:2104.07580](https://arxiv.org/abs/2104.07580) [stat.ME]
- [46] Massey Jr, F.J.: The kolmogorov-smirnov test for goodness of fit. *Journal of the American Statistical Association* **46**(253), 68–78 (1951)
- [47] Dimitrova, D.S., Kaishev, V.K., Tan, S.: Computing the kolmogorov-smirnov distribution when the underlying cdf is purely discrete, mixed, or continuous. *Journal of Statistical Software* **95**(1), 1–42 (2020)
- [48] An, K.: Sulla determinazione empirica di una legge didistribuzione. *Giorn Dell’inst Ital Degli Att* **4**, 89–91 (1933)
- [49] Marsaglia, G., Tsang, W.W., Wang, J., *et al.*: Evaluating kolmogorov’s distribution. *Journal of statistical software* **8**(18), 1–4 (2003)
- [50] Kryszicki, W., Bartos, J., Dyczka, W., Kr olikowska, K., Wasilewski, M.: *Rachunek prawdopodobie nstwa i statystyka matematyczna w zadaniach. Cz. II. Statystyka matematyczna*, PWN, Warszawa (1999)
- [51] Anderson, T.W.: Anderson–darling test. In: Dodge, Y. (ed.) *The Concise Encyclopedia of Statistics*, pp. 12–14. Springer, New York (2008). https://doi.org/10.1007/978-0-387-32833-1_11
- [52] Stephens, M.A.: Edf statistics for goodness of fit and some comparisons. *Journal of the American Statistical Association* **69**(347), 730–737 (1974)
- [53] Lewis, P.A.: Distribution of the anderson-darling statistic. *The Annals of Mathematical Statistics*, 1118–1124 (1961)
- [54] Marsaglia, G., Marsaglia, J.: Evaluating the anderson-darling distribution. *Journal of statistical software* **9**, 1–5 (2004)
- [55] Anderson, T.W.: Anderson–darling tests of goodness-of-fit. In: Lovric, M. (ed.) *International Encyclopedia of Statistical Science*, pp. 52–54. Springer, Berlin, Heidelberg (2011). https://doi.org/10.1007/978-3-642-04898-2_118
- [56] Schoutens, W.: *L vy Processes in Finance: Pricing Financial Derivatives*. John Wiley & Sons, West Sussex (2003)

Appendix A Iterative Maximum Likelihood Estimation (MLE) Procedure

Table A1: Convergence of the GTS parameter for Bitcoin return data

Iterations	μ	β_+	β_-	α_+	α_-	λ_+	λ_-	Log(ML)	$\ \frac{dLog(ML)}{d\theta}\ $	MaxEigenValue
1	-0.7369246	0.4613783	0.2671787	0.8100173	0.5173470	0.2156289	0.1919378	-10609.058	282.6765666	3.6240151
2	-0.7977019	0.4654390	0.2169392	0.7846817	0.4905332	0.2164395	0.2049523	-10607.253	26.7522215	-1.6194299
3	-0.4455841	0.3884721	0.3213867	0.7758150	0.5193395	0.2340187	0.1883953	-10607.001	50.1355291	3.0916011
4	-0.7634445	0.4521878	0.2217702	0.7935129	0.4959371	0.2218253	0.2055181	-10607.210	4.8235882	-2.6390063
5	-0.4906746	0.4146531	0.3404176	0.7722729	0.5222110	0.2269202	0.1846457	-10607.059	67.6646338	9.0971871
6	-0.5515834	0.4434827	0.3335905	0.7724484	0.5190619	0.2197566	0.1853686	-10607.022	17.4476962	-0.4021102
7	-0.4914586	0.4327714	0.3503012	0.7686883	0.5235361	0.2216450	0.1826269	-10606.991	16.2838831	-0.1781480
8	-0.2900908	0.3885350	0.3956186	0.7563357	0.5370260	0.2300772	0.1754994	-10606.864	12.0116477	-2.4090216
9	-0.2752698	0.3832660	0.3969704	0.7555456	0.5377367	0.2312224	0.1753571	-10606.847	11.4457840	-2.5487401
10	-0.2609339	0.3780400	0.3982456	0.7547812	0.5384209	0.2323632	0.1752258	-10606.832	10.8628213	-2.6874876
11	-0.2085409	0.3576927	0.4025762	0.7519966	0.5408864	0.2368544	0.1748113	-10606.782	8.3600783	-3.4356438
12	-0.1970109	0.3528575	0.4034002	0.7513923	0.5414138	0.2379362	0.1747455	-10606.772	7.6818408	-3.6954428
13	-0.1761733	0.3436416	0.4046818	0.7503191	0.5423414	0.2400174	0.1746675	-10606.756	6.2516380	-4.2766527
14	-0.1668421	0.3392794	0.4051522	0.7498492	0.5427438	0.2410120	0.1746529	-10606.750	5.5002876	-4.5807361
15	-0.1581860	0.3350854	0.4055256	0.7494209	0.5431090	0.2419740	0.1746517	-10606.745	4.7262048	-4.8824015
16	-0.1501600	0.3310612	0.4058166	0.7490311	0.5434404	0.2429024	0.1746615	-10606.741	3.9306487	-5.1742197
17	-0.1209376	0.3159301	0.4066945	0.7476393	0.5446224	0.2464122	0.1747326	-10606.734	2.8592342	-6.2251311
18	-0.1216487	0.3155707	0.4064438	0.7477179	0.5445608	0.2465247	0.1747753	-10606.734	0.0014787	-6.2014232
19	-0.1215714	0.3155483	0.4064635	0.7477142	0.5445652	0.2465296	0.1747719	-10606.734	1.82E-06	-6.2026532
20	-0.1215714	0.3155483	0.4064635	0.7477142	0.5445652	0.2465296	0.1747719	-10606.734	9.80E-10	-6.2026530

Table A2: Convergence of the GTS parameter for Ethereum return data

Iterations	μ	β_+	β_-	α_+	α_-	λ_+	λ_-	Log(ML)	$\ \frac{dLog(ML)}{d\theta}\ $	MaxEigenValue
1	-0.1215714	0.3155483	0.4064635	0.7477142	0.5445652	0.2465296	0.1747719	-9745.171	2673.428257	206.013602
2	-0.1724835	0.3319505	0.4091022	0.7364129	0.5479934	0.2227870	0.1684568	-9700.715	2388.609394	180.884105
3	-0.2041418	0.3384742	0.4118929	0.7338794	0.5531083	0.2083203	0.1632896	-9669.986	2139.267660	157.699659
4	-0.4006157	0.3530035	0.4393474	0.7513784	0.6172425	0.1135743	0.1221930	-9586.115	1471.570475	32.410140
5	-0.6485551	0.4493817	0.4404508	0.9247887	0.7210031	0.1412949	0.1482307	-9556.026	380.605737	56.584055
6	-0.6290525	0.4371402	0.4359516	0.9780784	0.7824777	0.1582340	0.1608694	-9553.005	24.905322	-0.719221
7	-0.5545412	0.3994778	0.3918188	0.9627486	0.7936571	0.1652438	0.1724287	-9552.866	5.834338	-0.847574
8	-0.4744837	0.3913982	0.4093404	0.9582366	0.8022858	0.1665103	0.1699928	-9552.862	2.963350	-0.933466
9	-0.4825586	0.3902160	0.4051365	0.9580755	0.8007651	0.1667400	0.1706850	-9552.862	0.214871	-0.931142
10	-0.4853678	0.3904369	0.4044899	0.9582486	0.8004799	0.1667119	0.1707853	-9552.862	0.004754	-0.931872
11	-0.4853800	0.3904362	0.4044846	0.9582487	0.8004779	0.1667121	0.1707862	-9552.862	2.96E-07	-0.931836
12	-0.4853800	0.3904362	0.4044846	0.9582487	0.8004779	0.1667121	0.1707862	-9552.862	1.18E-10	-0.931836
13	-0.4853800	0.3904362	0.4044846	0.9582487	0.8004779	0.1667121	0.1707862	-9552.862	1.27E-11	-0.931836

Table A3: Convergence of the GTS parameter for S&P 500 return data

Iterations	μ	β_+	β_-	α_+	α_-	λ_+	λ_-	Log(ML)	$\ \frac{dLog(ML)}{d\theta}\ $	MaxEigenValue
1	-0.2606426	0.34087979	0.02221141	0.78775729	0.59711061	1.28855513	1.01435308	-4921.0858	147.214541	-0.476265
2	-0.2747887	0.37848567	0.02517846	0.72538248	0.594628	1.22107935	1.01081205	-4920.9765	107.910271	-12.169518
3	-0.2852743	0.34562742	0.01628972	0.78353361	0.58024658	1.27423544	0.9888729	-4920.6236	23.70873	11.9588258
4	-0.2971254	0.37985815	0.05392593	0.74068472	0.55972179	1.22737986	0.96278568	-4920.5493	4.21443356	0.29705471
5	-0.3415082	0.42600675	0.0432239	0.69783497	0.56106365	1.18286494	0.966753	-4920.5722	37.0642417	-1.7903876
6	-0.2995817	0.40315129	0.12236507	0.7168274	0.522172	1.20383351	0.9117451	-4920.574	3.07232514	-0.7101089
7	-0.2944623	0.3977257	0.12218751	0.72174351	0.52260032	1.20899714	0.9121201	-4920.5701	2.63567879	-1.0187469
8	-0.2767429	0.37561063	0.11561097	0.7427615	0.52696799	1.23067384	0.91742165	-4920.5511	1.83311761	-2.1103436
9	-0.274204	0.37177939	0.11355883	0.74659763	0.52814335	1.2345524	0.91893546	-4920.5477	1.75839181	-2.177405
10	-0.2559812	0.34147926	0.09643312	0.77815581	0.53784221	1.26594249	0.93144448	-4920.5308	1.33811298	-2.6954121
11	-0.2496977	0.32954013	0.08928069	0.79125494	0.54186044	1.27868642	0.93662846	-4920.5291	0.79520373	-2.8166517
12	-0.2494237	0.32862462	0.08869445	0.79238161	0.54221561	1.27970094	0.93708759	-4920.5291	0.00166731	-2.6765739
13	-0.2494072	0.32862462	0.08864569	0.79242579	0.54224632	1.27974278	0.93712865	-4920.5291	0.00013552	-2.6768326
14	-0.2494082	0.32862428	0.08864047	0.79242619	0.54224944	1.27974312	0.93713293	-4920.5291	1.47E-05	-2.6766945
15	-0.2494083	0.32862424	0.08863992	0.79242624	0.54224977	1.27974315	0.93713338	-4920.5291	1.57E-06	-2.67668
16	-0.2494083	0.32862424	0.08863985	0.79242624	0.54224981	1.27974316	0.93713344	-4920.5291	1.89E-09	-2.6766783
17	-0.2494083	0.32862424	0.08863985	0.79242624	0.54224981	1.27974316	0.93713344	-4920.5291	2.09E-10	-2.6766783

Table A4: Convergence of the GTS parameter for SPY EFT return data

Iterations	μ	β_+	β_-	α_+	α_-	λ_+	λ_-	Log(ML)	$\ \frac{dLog(ML)}{d\theta}\ $	MaxEigenValue
1	-0.0518661	0.1161846	0.2186548	1.04269292	0.52712574	1.52244991	0.91168779	-4894.2279	14.7801725	-6.5141947
2	-0.1102477	0.18491276	0.17478472	0.94756655	0.52844271	1.4399315	0.91415148	-4893.8278	29.8166141	-1.9290981
3	-0.2094204	0.29377592	0.0891446	0.84029122	0.56054563	1.34797271	0.96500981	-4893.3554	16.9940095	4.33892902
4	-0.1985664	0.29758208	0.13230013	0.83156167	0.53656079	1.33833078	0.93230856	-4893.4206	10.9048744	1.04588745
5	-0.078883	0.25939922	0.39611543	0.84865673	0.40365522	1.35595932	0.7410936	-4895.8806	241.028178	94.6293224
6	-0.0753571	0.26704857	0.33754158	0.84120908	0.45446164	1.3452823	0.80751063	-4894.3899	25.1995505	-2.805571
7	-0.196642	0.31624372	0.20068543	0.80509106	0.50322368	1.30837612	0.88967028	-4893.888	140.257551	34.770691
8	-0.1898283	0.3045047	0.15900291	0.81380451	0.52672075	1.31341912	0.91775259	-4893.4694	6.29433991	-4.6080872
9	-0.2275214	0.32940996	0.10770535	0.79340215	0.55020025	1.29360449	0.95260474	-4893.3049	7.34361008	-8.1891832
10	-0.2726283	0.34972465	0.01601222	0.78061523	0.59736004	1.28153304	1.01757433	-4893.2192	14.0784211	-3.6408772
11	-0.2499816	0.32645286	0.01851524	0.80217301	0.60018154	1.30243672	1.01792703	-4893.2125	6.27794755	-4.6455546
12	-0.2575953	0.33832596	0.02643321	0.79008383	0.59450637	1.29085215	1.01101001	-4893.208	1.23298227	-6.8035318
13	-0.2607071	0.34052644	0.02075252	0.78817075	0.59805376	1.28895161	1.01555438	-4893.2076	0.07363298	-6.71708
14	-0.2606368	0.34088815	0.02227012	0.78774693	0.59707082	1.28854532	1.01430383	-4893.2076	0.00156771	-6.6908109
15	-0.2606432	0.34087911	0.02220633	0.78775813	0.59711397	1.28855593	1.01435731	-4893.2076	0.00010164	-6.6915902
16	-0.2606426	0.34087985	0.02221188	0.78775721	0.59711103	1.28855506	1.01435268	-4893.2076	8.45E-06	-6.6915177
17	-0.2606426	0.34087979	0.02221141	0.78775729	0.59711061	1.28855513	1.01435308	-4893.2076	7.21E-07	-6.6915239

Appendix B Pearson Statistic Inputs

Table B1: Observed versus Expected statistics under GTS distribution

k	Bitcoin			Ethereum			sp500			SPY EFT		
	x(k)	n* Π_k	n(k)	x(k)	n* Π_k	n(k)	x(k)	n* Π_k	n(k)	x(k)	n* Π_k	n(k)
1	-18.988	7.512	8	-20.861	7.531	6	-4.341	10.264	12	-4.405	8.327	11
2	-17.080	4.144	7	-18.321	5.583	6	-3.935	5.456	5	-4.007	4.562	3
3	-15.172	6.603	7	-15.781	10.018	15	-3.529	8.442	7	-3.608	7.116	7
4	-13.264	10.678	9	-13.241	18.331	20	-3.123	13.138	15	-3.210	11.144	12
5	-11.356	17.586	13	-10.700	34.424	29	-2.717	20.588	20	-2.811	17.538	18
6	-9.448	29.661	32	-8.160	66.980	68	-2.311	32.543	30	-2.413	27.775	27
7	-7.540	51.657	47	-5.620	137.268	134	-1.905	52.023	48	-2.015	44.350	41
8	-5.632	94.188	107	-3.080	305.591	305	-1.499	84.479	89	-1.616	71.617	73
9	-3.724	184.486	168	-0.540	769.951	769	-1.093	140.406	147	-1.218	117.552	122
10	-1.816	411.503	419	2.000	965.210	966	-0.687	242.564	244	-0.819	198.101	186
11	0.092	1195.725	1186	4.540	458.955	466	-0.281	455.971	456	-0.421	351.660	348
12	2.000	1150.470	1159	7.080	219.873	222	0.126	896.809	896	-0.023	725.476	730
13	3.908	473.177	469	9.620	111.760	101	0.532	749.106	733	0.376	867.735	867
14	5.816	217.783	227	12.160	59.253	60	0.938	430.841	426	0.774	541.022	522
15	7.724	107.387	102	14.700	32.379	32	1.344	234.692	260	1.173	300.464	325
16	9.632	55.272	51	17.241	18.099	21	1.750	126.820	137	1.571	163.491	189
17	11.540	29.294	39	19.781	10.296	12	2.156	68.688	57	1.969	88.862	82
18	13.448	15.861	14	22.321	5.939	5	2.562	37.387	33	2.368	48.491	36
19	15.356	8.729	9	24.861	3.465	5	2.968	20.460	15	2.766	26.600	23
20	17.264	4.866	4		5.091	4	3.374	11.256	12	3.165	14.669	13
21		6.419	6					14.067	14		18.450	20

Appendix C Bitcoin BTC : Kobl distribution ($\beta = \beta_- = \beta_+$)

$$V(dx) = \left(\alpha_+ \frac{e^{-\lambda_+ x}}{x^{1+\beta}} \mathbf{1}_{x>0} + \alpha_- \frac{e^{-\lambda_- |x|}}{|x|^{1+\beta}} \mathbf{1}_{x<0} \right) dx \quad (C1)$$

$$\Psi(\xi) = \mu \xi i + \Gamma(-\beta) \left[\alpha_+ ((\lambda_+ - i\xi)^\beta - \lambda_+^\beta) + \alpha_- ((\lambda_- + i\xi)^\beta - \lambda_-^\beta) \right] \quad (C2)$$

Table C1: Kobl maximum-likelihood estimation for Bitcoin return data

Model	Parameter	Estimate	Std Err	\mathbf{z}	$Pr(Z > z)$	[95% Conf.Interval]	
GTS	μ	-0.292833	(0.126)	-2.32	2.1E-02	-0.541	-0.045
	β	0.367074	(0.086)	4.27	1.9E-05	0.199	0.535
	α_+	0.755914	(0.047)	16.02	4.7E-58	0.663	0.848
	α_-	0.535121	(0.034)	15.68	9.6E-56	0.468	0.602
	λ_+	0.235266	(0.027)	8.87	3.6E-19	0.183	0.287
	λ_-	0.181602	(0.023)	7.94	9.8E-16	0.137	0.226
	Log(ML)		-10607				
AIC		21226					
BIK		21264					

Table C2: Convergence of the Kobl parameter for Bitcoin return data

Iterations	μ	β	α_+	α_-	λ_+	λ_-	$Log(ML)$	$\ \frac{dLog(ML)}{d\theta}\ $	MaxEigenValue
1	-0.1215714	0.3155483	0.7477142	0.5445652	0.2465296	0.17477186	-10614.93879	450.0556974	25.6678081
2	-0.255172	0.36516958	0.73215119	0.53194253	0.22955186	0.17909072	-10607.01058	51.74982347	-46.893383
3	-0.2912276	0.37096854	0.75410108	0.53529439	0.23387716	0.18070591	-10606.81236	1.484798964	-53.728563
4	-0.2922408	0.36574333	0.7559582	0.53508403	0.23560819	0.18189913	-10606.81041	0.258928464	-53.391237
5	-0.2928641	0.36714311	0.75591147	0.53512239	0.23524801	0.18158588	-10606.81025	0.01286122	-53.406734
6	-0.292837	0.36708319	0.75591382	0.53512107	0.23526357	0.18159941	-10606.81025	0.00174219	-53.40643
7	-0.2928328	0.36707373	0.75591419	0.53512086	0.23526603	0.18160154	-10606.81025	1.18E-05	-53.406384
8	-0.2928328	0.36707379	0.75591419	0.53512086	0.23526602	0.18160153	-10606.81025	1.60E-06	-53.406384
9	-0.2928328	0.36707379	0.75591419	0.53512086	0.23526601	0.18160153	-10606.81025	2.18E-07	-53.406384
10	-0.2928328	0.36707379	0.75591419	0.53512086	0.23526601	0.18160153	-10606.81025	1.09E-08	-53.406384

Appendix D Ethereum: Carr-Geman-Madan-Yor (CGMY) distributions

$$V(dx) = \left(\alpha \frac{e^{-\lambda_+ x}}{x^{1+\beta}} \mathbf{1}_{x>0} + \alpha \frac{e^{-\lambda_- |x|}}{|x|^{1+\beta}} \mathbf{1}_{x<0} \right) dx \quad (D1)$$

$$\Psi(\xi) = \mu \xi i + \alpha \Gamma(-\beta) \left[((\lambda_+ - i\xi)^\beta - \lambda_+^\beta) + ((\lambda_- + i\xi)^\beta - \lambda_-^\beta) \right] \quad (D2)$$

Table D1: CGMY maximum-likelihood estimation for Ethereum return data

Model	Parameter	Estimate	Std Err	\mathbf{z}	$Pr(Z > z)$	[95% Conf.Interval]	
GTS	μ	-0.147089	(0.079)	-1.86	6.3E-02	-0.302	-0.008
	β	0.398418	(0.127)	3.12	1.8E-03	0.148	0.649
	α	0.887161	(0.058)	15.22	1.2E-52	0.773	1.001
	λ_+	0.155369	(0.023)	6.56	5.2E-11	0.109	0.202
	λ_-	0.185991	(0.025)	7.29	2.9E-13	0.136	0.236
	Log(ML)	-9554					
	AIC	19118					
BIK	19149						

Table D2: Convergence of the CGMY parameter for Ethereum return data

Iterations	μ	β	α	λ_+	λ_-	$Log(ML)$	$\left\ \frac{dLog(ML)}{dV} \right\ $	$MaxEigenValue$
1	-0.48538	0.39043616	0.95824875	0.16671208	0.17078617	-9596.2658	1653.57149	-140.21456
2	-0.0545131	0.40148247	0.88205674	0.15875317	0.18060554	-9554.6834	80.0921993	-19.637869
3	-0.1479632	0.39049434	0.88271998	0.15631408	0.18704084	-9553.9065	3.84112398	-44.76325
4	-0.1465893	0.40345482	0.88868927	0.15450383	0.18507239	-9553.9036	0.4436942	-55.029934
5	-0.1472464	0.39683622	0.88667597	0.15564017	0.18628001	-9553.9026	0.14094418	-51.274906
6	-0.1470247	0.39907668	0.88736036	0.15525581	0.18587143	-9553.9025	0.05563606	-52.523819
7	-0.1471148	0.39816841	0.88708569	0.15541227	0.18603772	-9553.9025	0.02143506	-52.017698
8	-0.1470898	0.39842098	0.88716234	0.15536883	0.18599155	-9553.9025	0.00019543	-52.158334
9	-0.14709	0.39841855	0.88716161	0.15536924	0.18599199	-9553.9025	1.16E-05	-52.156981
10	-0.14709	0.39841867	0.88716164	0.15536922	0.18599197	-9553.9025	1.78E-06	-52.157046
11	-0.14709	0.39841869	0.88716165	0.15536922	0.18599197	-9553.9025	2.71E-07	-52.157055
12	-0.14709	0.39841869	0.88716165	0.15536922	0.18599197	-9553.9025	4.14E-08	-52.157057

Appendix E S&P 500 index: Bilateral Gamma (BG) distribution ($\beta_- = \beta_+ = 0$)

$$V(dx) = \left(\alpha_+ \frac{e^{-\lambda_+ x}}{x} \mathbf{1}_{x>0} + \alpha_- \frac{e^{-\lambda_- |x|}}{|x|} \mathbf{1}_{x<0} \right) dx \quad (\text{E1})$$

$$\Psi(\xi) = \mu \xi i - \alpha_+ \log \left(1 - \frac{1}{\lambda_+} i \xi \right) - \alpha_- \log \left(1 + \frac{1}{\lambda_-} i \xi \right) \quad (\text{E2})$$

Table E1: BG maximum-likelihood estimation for S&P 500 return data

Model	Parameter	Estimate	Std Err	\mathbf{z}	$Pr(Z > z)$	[95% Conf.Interval]	
GTS	μ	-0.031467	(0.010)	-3.07	2.1E-03	-0.052	-0.011
	α_+	1.092741	(0.058)	18.98	2.6E-80	0.980	1.206
	α_-	0.701784	(0.042)	16.80	2.3E-63	0.620	0.784
	λ_+	1.539690	(0.064)	22.82	3.1E-115	1.407	1.672
	λ_-	1.110737	(0.050)	22.07	6.6E-108	1.012	1.209
	Log(ML)	-4925					
	AIC	9859					
BIK	9890						

Table E2: Convergence of the BG parameter for S&P 500 return data

<i>Iterations</i>	μ	α_+	α_-	λ_+	λ_-	$Log(ML)$	$\ \frac{dLog(ML)}{dV} \ $	<i>MaxEigenValue</i>
1	0	0.79242624	0.54224981	1.27974316	0.93713344	-4951.1439	1138.53458	-265.251
2	-0.0038447	0.93153413	0.64461254	1.41132138	1.05504868	-4931.7583	549.025405	-171.22804
3	-0.0103214	1.03062846	0.70198868	1.49426667	1.10555794	-4926.8412	286.215345	-126.18156
4	-0.0186317	1.07922912	0.71421996	1.53377391	1.11392285	-4925.393	135.694287	-113.12071
5	-0.0279475	1.09450205	0.70493092	1.54418172	1.10795103	-4924.7065	38.0551545	-116.58686
6	-0.0313951	1.09325663	0.70162581	1.54038766	1.10996346	-4924.621	1.54417452	-120.06271
7	-0.0314671	1.09274119	0.70178365	1.53969027	1.11073682	-4924.6205	0.02788236	-120.35435
8	-0.0314664	1.09276971	0.70182788	1.53971127	1.11079928	-4924.6205	0.00198685	-120.34482
9	-0.0314663	1.09277213	0.70183158	1.5397131	1.11080431	-4924.6205	0.00016039	-120.34394
10	-0.0314662	1.09277232	0.70183188	1.53971325	1.11080472	-4924.6205	1.29E-05	-120.34387
11	-0.0314662	1.09277234	0.7018319	1.53971326	1.11080475	-4924.6205	1.04E-06	-120.34387
12	-0.0314662	1.09277234	0.7018319	1.53971326	1.11080476	-4924.6205	8.43E-08	-120.34387
13	-0.0314662	1.09277234	0.7018319	1.53971326	1.11080476	-4924.6205	6.80E-09	-120.34387
14	-0.0314662	1.09277234	0.7018319	1.53971326	1.11080476	-4924.6205	5.63E-10	-120.34387
15	-0.0314662	1.09277234	0.7018319	1.53971326	1.11080476	-4924.6205	5.73E-11	-120.34387

Appendix F SPY ETF: Bilateral Gamma (BG) distribution ($\beta_- = \beta_+ = 0$)

$$V(dx) = \left(\alpha_+ \frac{e^{-\lambda_+ x}}{x} \mathbf{1}_{x>0} + \alpha_- \frac{e^{-\lambda_- |x|}}{|x|} \mathbf{1}_{x<0} \right) dx \quad (\text{F1})$$

$$\Psi(\xi) = \mu \xi i - \alpha_+ \log \left(1 - \frac{1}{\lambda_+} i \xi \right) - \alpha_- \log \left(1 + \frac{1}{\lambda_-} i \xi \right) \quad (\text{F2})$$

Table F1: BG maximum-likelihood estimation for SPY EFT return data

Model	Parameter	Estimate	Std Err	\mathbf{z}	$Pr(Z > z)$	[95% Conf.Interval]		
GTS	μ	0.015048	(0.012)	1.28	2.0E-01	-0.008	0.038	
	α_+	1.068239	(0.067)	16.02	8.6E-58	0.938	1.199	
	α_-	0.764449	(0.044)	17.33	3.0E-67	0.678	0.851	
	λ_+	1.525718	(0.073)	20.98	1.1E-97	1.383	1.668	
	λ_-	1.156439	(0.052)	22.15	1.1E-108	1.054	1.259	
	Log(ML)		-4899					
	AIC		9807					
BIK		9838						

Table F2: Convergence of the BG parameter for SPY EFT return data

Iterations	μ	α_+	α_-	λ_+	λ_-	Log(ML)	$\left\ \frac{dLog(ML)}{dV} \right\ $	MaxEigenValue
1	0	0.78775729	0.59711061	1.28855513	1.01435308	-4918.7331	406.35365	-252.28104
2	0.02867773	0.97562263	0.67572827	1.46822249	0.97596762	-4908.5992	226.190986	-116.11753
3	0.02727407	1.05127517	0.78618306	1.51846501	1.17883595	-4899.0798	45.2281041	-96.788275
4	0.00834089	1.07692251	0.75226045	1.5348003	1.14577232	-4898.9955	131.637516	-107.77617
5	0.01126962	1.07242358	0.7568497	1.53011913	1.1494212	-4898.751	48.0005418	-103.03258
6	0.01386478	1.06933921	0.76167668	1.52688303	1.15363987	-4898.6763	11.3246873	-100.1483
7	0.01492745	1.06823047	0.76397541	1.52573245	1.15588409	-4898.6693	0.98802026	-99.171136
8	0.01504464	1.06821119	0.76439389	1.52569528	1.15636567	-4898.6693	0.02529683	-99.040575
9	0.01504742	1.06823539	0.76444163	1.5257152	1.15642976	-4898.6693	0.00300624	-99.030178
10	0.01504762	1.06823881	0.76444764	1.52571803	1.15643796	-4898.6693	0.00038489	-99.028926
11	0.01504764	1.06823925	0.76444841	1.52571839	1.15643901	-4898.6693	4.92E-05	-99.028765
12	0.01504765	1.06823931	0.76444851	1.52571844	1.15643915	-4898.6693	6.30E-06	-99.028745
13	0.01504765	1.06823932	0.76444852	1.52571845	1.15643917	-4898.6693	1.32E-08	-99.028742
14	0.01504765	1.06823932	0.76444852	1.52571845	1.15643917	-4898.6693	1.69E-09	-99.028742
15	0.01504765	1.06823932	0.76444852	1.52571845	1.15643917	-4898.6693	2.23E-10	-99.028742